



**HAL**  
open science

## Rb-Sr constraints on the age of Moon formation

Elsa Yobregat, Caroline Fitoussi, Bernard Bourdon

► **To cite this version:**

Elsa Yobregat, Caroline Fitoussi, Bernard Bourdon. Rb-Sr constraints on the age of Moon formation. *Icarus*, 2024, 420, pp.116164. 10.1016/j.icarus.2024.116164 . hal-04778395

**HAL Id: hal-04778395**

**<https://hal.science/hal-04778395v1>**

Submitted on 13 Nov 2024

**HAL** is a multi-disciplinary open access archive for the deposit and dissemination of scientific research documents, whether they are published or not. The documents may come from teaching and research institutions in France or abroad, or from public or private research centers.

L'archive ouverte pluridisciplinaire **HAL**, est destinée au dépôt et à la diffusion de documents scientifiques de niveau recherche, publiés ou non, émanant des établissements d'enseignement et de recherche français ou étrangers, des laboratoires publics ou privés.

# Rb-Sr constraints on the age of Moon formation

Elsa Yobregat<sup>1</sup>, Caroline Fitoussi<sup>1</sup>, Bernard Bourdon\*<sup>1</sup>

<sup>1</sup> Laboratoire de Géologie de Lyon, ENS Lyon, CNRS and UCBL

\*Correspondence to: [bernard.bourdon@ens-lyon.fr](mailto:bernard.bourdon@ens-lyon.fr)

**Keywords: Moon, Strontium isotopes, chronology, anorthosite**

## Abstract:

Determining the age of the Moon, which is commonly considered as the termination of Earth accretion has been a complex challenge for geochronology. A number of methods have been used to delineate the age of the Moon based either on absolute chronology of lunar rocks or have relied on more indirect methods using short-lived nuclides such as <sup>182</sup>Hf that was present in the early history of the Solar System. Model ages usually require some assumptions that are sometimes controversial or harder to verify.

In this study, new high precision Sr isotope data (2.4 ppm, 2SD) were obtained for a well-dated lunar anorthosite (60025) in order to better constrain the initial <sup>87</sup>Sr/<sup>86</sup>Sr of the bulk silicate Moon. This new data is then used to model the Sr isotope evolution of the Earth-Moon starting from the beginning of the Solar System. To comply with the Hf-W and stable isotope constraints, we then assume that the Earth and Moon were equilibrated at the time of Moon formation. By investigating systematically all the sources of uncertainties in our model, we show that compared with previous work on anorthosite, one can tighten the constraints on the youngest age of Moon formation to no more than 79 Ma after the beginning of the Solar System, i.e. the Moon cannot be younger than 4488 Ma.

## Highlights:

- New high precision Sr isotope data yields a constraint on Moon formation.
- The youngest age of the Moon is 79 Ma after the beginning of the Solar System.
- This model age includes all sources of uncertainties using MonteCarlo simulations.

## 1. Introduction

32           The Moon is thought to have formed after the collision of a large planetary object with the  
33 proto-Earth, yielding a disk of vapor and liquid that later accreted the Moon. Obtaining a reliable  
34 constraint on the age of this event has proven difficult, due to the absence of lunar rocks or minerals  
35 directly recording this event. An indirect approach based on the  $^{182}\text{Hf}$ - $^{182}\text{W}$  isotope system  
36 (Touboul et al., 2007) was used to argue that the Moon should have formed at least 45 Ma after  
37 the beginning of the Solar System based on the observation that the  $^{182}\text{W}$  abundance in the Moon  
38 and the Earth were almost identical, despite having a difference between Hf/W ratios in lunar and  
39 terrestrial rocks. This approach was questioned by König et al. (2011) and (Münker, 2010) who  
40 argued that the Moon and Earth had almost identical Hf/W ratios, which implies that no  $^{182}\text{W}$   
41 difference would be expected between the Moon and the Earth, if they initially formed from the  
42 same material. Subsequently, the studies of Touboul et al. (2015) and (Kruijer et al. (2015) have  
43 shown that there was a small ( $\approx 15$  ppm) but resolvable difference between Moon and Earth in  $^{182}\text{W}$   
44 abundances. However, this difference was ascribed to different proportions of late accreted  
45 material between Moon and Earth. More recently, Thiemens et al. (2019) have shown that reliable  
46 Hf/W ratios for the bulk Silicate Moon can only be obtained using low-Ti basalts, as high-Ti  
47 basalts have saturated metal and Ti-rich phases, which makes an estimate of their Hf/W source  
48 difficult. On this basis, the observed Hf/W ratios of low-Ti basalts ranging between 30-48 was  
49 used to infer the Hf/W ratio of the bulk silicate Moon (BSM), which proved significantly higher  
50 than that of the BSE (26); this difference between the Moon and the bulk silicate Earth was then  
51 used to determine an  $^{182}\text{Hf}$ - $^{182}\text{W}$  age for the Moon formation of 50 Ma based on the observed small  
52 15 ppm difference in  $^{182}\text{W}$  abundance between Moon and Earth (Kruijer et al., 2015; Touboul et  
53 al., 2015). In that study, however, it was considered that the excess  $^{182}\text{W}$  was not related to late  
54 accretion. The small difference in  $^{182}\text{W}$  abundance between present-day Earth and Moon was then  
55 interpreted as reflecting in-growth of  $^{182}\text{W}$  in the Bulk Silicate Moon (BSM) relative to the BSE  
56 and a range of Moon formation ages between 45 and 60 Ma was inferred (Thiemens et al., 2019).  
57 However, this age determination was questioned by Kruijer et al. (2021) who showed that if one  
58 takes into account the possible difference between HSE budget between Earth and Moon, then  
59 there is no longer a difference in  $^{182}\text{W}$  abundance between Earth and Moon, which means that the  
60 Hf-W constraints on the age of the Moon indicates that it must have formed later than  $\approx 50$  Ma  
61 (upper limit), as originally inferred in Touboul et al. (2007), even though the constraints on the  
62 Hf/W ratio in the BSM and BSE are admittedly not very tight.

63 Using a very different approach, Jacobson et al. (2014) demonstrated that the mass of  
64 material accreted to the Earth after the Moon-forming impact, the so-called ‘late veneer’ was a  
65 function of the time at which the Moon formed. This is simply because the mass of objects in the  
66 protoplanetary disk available to accrete to Earth is decaying with time. Thus, by measuring the  
67 abundance of highly siderophile elements in the Earth’s mantle, which is a proxy for the mass of  
68 late accreted material, it is possible to constrain an age for the Moon formation to be  $95\pm 32$  Ma at  
69 the earliest after the beginning of the Solar System. This approach has been reasserted by recent  
70 work showing the unfractionated and homogeneous HSE pattern in mantle derived rocks (e.g.  
71 Paquet et al. 2023) that is consistent with late accretion, rather than intra-mantle processes (see  
72 also Righter et al. 2023). Using a completely different method, Barboni et al. (2017) have argued  
73 that Hf isotope data for lunar zircons suggest that the Moon was already differentiated  $58\pm 20$  Ma  
74 after the start of the Solar System and that the Moon must have formed before that time. However,  
75 this age determination has been questioned in the study of Borg and Carlson (2023) who argued  
76 that this data set was not consistent with earlier work on whole rocks (Gaffney and Borg 2014;  
77 Sprung et al. 2013) or with earlier Lu-Hf data on zircons (Taylor et al. 2009).

78 Based on internal isochrons obtained for ferroanorthosite rock 60025, Borg et al. (2011)  
79 obtained a consistent  $^{146}\text{Sm}-^{142}\text{Nd}$ ,  $^{143}\text{Nd}-^{147}\text{Sm}$  and U-Pb age for ferroanorthosite rock 60025. If  
80 there had been a magma ocean in the history of the Moon, this age would indicate that the  
81 formation of anorthositic crust of the Moon lasted at least until 200 Myr after the beginning of the  
82 Solar System (see also Borg et al., 2020, 2019, 2011). Whether these anorthosite ages accurately  
83 represent the age of the Moon is a matter of debate. At the very least, the anorthosites that represent  
84 the oldest rocks found on the Moon give the youngest bound for the age of Moon formation. If one  
85 argues furthermore that the magma ocean was short-lived (at most 10 Ma, according to Elkins-  
86 Tanton et al., 2011), this age would indicate that the Moon would have formed only shortly before  
87 that. To reconcile this young age for the Moon with the relatively older sets of ages, several models  
88 for a long duration of the lunar magma ocean (LMO) have been proposed, with the latest version  
89 proposing a preferred model where the magma ocean crystallization stopped 170 Myr after  
90 accretion (Maurice et al., 2020). This study combining a thermal model with geochronological  
91 constraints concludes that the age of the Moon should be  $143\pm 25$  Myr after the start of the Solar  
92 System. A more recent study has found that zircons from Apollo 17 impact melt breccia yielded  
93 U-Pb ages as old as  $4460\pm 31$  Ma (Zhang et al., 2021), which yields an age of Moon formation at

94 107 Ma or earlier. Last, Connelly and Bizzarro (2016) have used the Pb isotope composition of  
95 the bulk silicate Earth to constrain the time of the Moon-forming impact indirectly and obtained a  
96 Pb model age as young as 4424-4417 Ma or 144-151 Ma after the beginning of the Solar System.  
97 Thus, there is a strong debate, that is still open, regarding the age of the Moon with some  
98 proponents for an ‘Old Moon’ based on Hf-W-HSE budgets, while the Sm-Nd/Lu-Hf U-Pb  
99 chronology of lunar rocks and thermal models would rather argue for a ‘Young Moon’.

100 By assuming that the Sr initial isotope composition of the Solar System is known and that  
101 the Rb/Sr ratio of the Earth-Moon system is identical to that of the bulk Silicate Earth, Halliday  
102 (2008) calculated an age for the formation of the Moon that ranged between 50 and 100 Ma, if one  
103 considers the total uncertainties in Rb/Sr and  $^{87}\text{Sr}/^{86}\text{Sr}$  ratios. Using a similar approach based on a  
104 two-component model for the Earth, Mezger et al. (2021) reported an age range between 45 and  
105 75 Myr. More recently, Borg et al. (2022) used published Rb-Sr data on lunar rocks to derive  
106 constraints on both the age of the Moon and the volatile evolution of Earth and Moon building  
107 blocks. Their conclusions were that Theia (i.e. the Moon-forming impactor) and the proto-Earth  
108 must have formed from precursors that were already depleted in moderately volatile elements such  
109 as Rb. In their scenario, the Moon could have formed from 90% of a highly Rb-depleted precursor  
110 mixed with 10% of proto-Earth material. By assuming that proto-Earth and Theia did not  
111 equilibrate isotopically at the time of the impact, the age of the Moon can be as late as 137 Ma  
112 after the beginning of the Solar System (e.g. Table S1, Model 6). These conclusions relied on the  
113 hypothesis that Theia and proto-Earth were made of isotopically similar materials in terms of Ti,  
114 Cr and O isotopes (as in Dauphas et al., 2014), arguing that these bodies must have both come  
115 from the same reservoirs in the inner Solar System.

116 Here, we have measured precisely the initial  $^{87}\text{Sr}/^{86}\text{Sr}$  of ferroanorthosite 60025 and  
117 revisited these interpretations, thereby providing a new view on Rb-Sr systematics of the Earth-  
118 Moon system. In this study, all the ages (unless specified) are reported relative to the beginning of  
119 the Solar System represented by the age of Calcium-Aluminium rich inclusions (CAI) dated at  
120 4567 Ma (Amelin et al., 2010; Connelly et al. 2012) with the U-Pb method.

121

## 122 **2. Methods**

### 123 *2.1 Sample preparation and Sr separation*

124 The 60025 rock is a pristine coarse-grained ferroan anorthosite from the lunar highlands sampled  
125 during the Apollo 16 mission. This sample is a breccia that is thought to come from ejecta from  
126 surrounding large impact basins. Thus, FAN 60025 represents a plutonic rock cooled at depth that  
127 must have been brought to the surface from a depth possibly as large as 50 km (e.g. Spudis et al.  
128 1989). The fragment analyzed in this study is nearly composed of pure plagioclase with only a few  
129 percent of mafic minerals. The sample was first coarsely crushed in an agate mortar, then mafic  
130 minerals, olivines, pyroxenes and oxides were handpicked under a binocular microscope. The  
131 plagioclase fraction (281.4 mg) was crushed into a fine powder and dissolved in a Savillex PFA  
132 beaker using an HF: HNO<sub>3</sub> mixture. The sample was then dried down and dissolved several times  
133 in concentrated HCl to remove fluorides.

134 The solution was loaded in 6 M HCl on a column filled with AG1 X8 (100-200 mesh size) anionic  
135 resin to remove Fe, which was retained in the column, while Sr was directly eluted. The sample  
136 was converted to nitrate form, then loaded in 3 M HNO<sub>3</sub> on 0.5 ml of Eichrom Sr-resin<sup>TM</sup>. Matrix  
137 elements, including Rb, were eluted in 2.5 ml of 3 M HNO<sub>3</sub>, then Ba was stripped from the resin  
138 with 6.5 ml of 7.5 M HNO<sub>3</sub> and finally Sr was collected with 10 ml of 0.05 M HNO<sub>3</sub>. The Sr  
139 fraction was evaporated and redissolved in aqua regia several times to remove traces of organic  
140 material released from the Sr-resin. The whole procedure yielded Sr blanks less than 30 ± 5 pg and  
141 Rb blanks <45 pg (representing less than 10% of the Rb present in the aliquot used for measuring  
142 Rb). The Rb and Sr concentrations were measured on a ~20 mg aliquot using a Thermo Element  
143 high-resolution ICP-MS. This instrument has very low detection level (~20 ppt) required to  
144 measure the very low Rb content of ferroan anorthosites.

145

## 146 *2.2 Mass spectrometric measurements of Sr isotope ratios*

147 The <sup>87</sup>Sr/<sup>86</sup>Sr ratios were measured on a Thermo Triton plus thermal ionization mass spectrometer  
148 following the methodology described in Yobregat et al. (2017). Approximately 1 µg of Sr was  
149 loaded onto single outgassed zone-refined Re filaments with a TaCl<sub>5</sub> activator. Intensities of  
150 10×10<sup>-11</sup> A for <sup>88</sup>Sr were maintained for at least 8 hours. Measurements were done in a  
151 multidynamic mode with the following Faraday cup configuration: <sup>85</sup>Rb (Axial), <sup>86</sup>Sr (H1), <sup>87</sup>Sr  
152 (H2), <sup>88</sup>Sr (H3) for line 1, <sup>85</sup>Rb (L1), <sup>86</sup>Sr (Axial), <sup>87</sup>Sr (H1), <sup>88</sup>Sr (H2) for line 2 and <sup>85</sup>Rb (L2),  
153 <sup>86</sup>Sr (L1), <sup>87</sup>Sr (Axial), <sup>88</sup>Sr (H1) for line 3. One run consisted of ~800 cycles with an 8 s integration

154 time for each line separated by a 5 s idle time. Amplifier rotation was used to improve uncertainties  
155 in final isotope ratios.

156 The NIST SRM 987 standard was measured over the course of this study and yielded a value of  
157  $0.7102487 \pm 0.0000044$  (0.6 ppm, 2 S.E.,  $n = 15$ ). It is common practice to use the 2SD reported  
158 for the standard values to determine the external reproducibility equal to 2.4 ppm (Table S1). The  
159  $^{87}\text{Sr}/^{86}\text{Sr}$  multidynamic ratios and  $^{87}\text{Rb}/^{86}\text{Sr}$  ratios for 60025 are listed in Table S2 and the data of  
160 Carlson and Lugmair (1988) for the same sample is reported for reference. The external  
161 reproducibility of 2.4 ppm (2 S.D.) achieved for the  $^{87}\text{Sr}/^{86}\text{Sr}$  ratio is about an order of magnitude  
162 better than the uncertainty of  $\sim 30$  ppm previously reported for the same sample (Carlson and  
163 Lugmair, 1988) and a factor of 5 compared with the uncertainty reported in Borg et al. (2022) for  
164 the same sample. For the calculations, we have used the external reproducibility (2SD) obtained  
165 on the NIST 987 standard equal to 2.4 ppm. The ICP-MS measurement of Rb and Sr concentrations  
166 used in this study is less precise than the conventional isotope dilution method, but the values are  
167 identical within error (5 %) to the isotope dilution concentrations given by Carlson and Lugmair  
168 (1988).

169

### 170 **3. Sr isotope evolution of ferroanorthosite 60025 and the initial $^{87}\text{Sr}/^{86}\text{Sr}$ ratio of the bulk** 171 **silicate Moon**

172 As shown in Table S2, we measured with high precision the  $^{87}\text{Sr}/^{86}\text{Sr}$  ratio of ferroanorthosite  
173 (FAN) 60025 that has been well characterized in previous studies (Borg et al., 2011; Carlson and  
174 Lugmair, 1988) and obtained a mean value of  $0.6990812 \pm 0.0000009$  (2 S.D.,  $n = 3$ , Table S2)  
175 using the analytical technique developed in Yobregat et al. (2017). If one uses the external  
176 reproducibility derived by NIST 987 measurements, the relative uncertainty obtained for the  
177 plagioclase fraction was thus equal to 2.4 ppm (2 S.D.). In comparison the measured  $^{87}\text{Sr}/^{86}\text{Sr}$  of  
178 the plagioclase fractions measured by Carlson and Lugmair (1988) was equal to 0.699096 and had  
179 a relative uncertainty of 28 ppm. If corrected for the difference in NIST 987 standard reported in  
180 Carlson and Lugmair (1988), this value is equal to 0.699085. The initial  $^{87}\text{Sr}/^{86}\text{Sr}$  ratio of FAN  
181 60025 at the time of its formation taken to be equal to 4.360 Ga (Borg et al., 2011) was calculated  
182 to be  $0.699063 \pm 0.0000019$ , using error propagation and assuming a 5% uncertainty on the Rb  
183 concentration (the  $^{87}\text{Rb}$  decay correction increases the uncertainty from 2.4 to 2.8 ppm). Note that  
184 the age of Borg et al. (2011) was chosen rather than that of Carlson and Lugmair (1988) as it was

185 consistent for three chronometers and also consistent with the age of other FANs (e.g. Borg and  
 186 Carlson 2023). All these methods yielded consistent isochron ages with a preferred value of  
 187  $4360 \pm 3$  Ma, which can be used to pin down the  $^{87}\text{Sr}/^{86}\text{Sr}$  of the FAN 60025 at the time this rock  
 188 formed. It is thus possible to calculate the initial  $^{87}\text{Sr}/^{86}\text{Sr}$  ratios of the mantle reservoir from which  
 189 this rock was derived at the time of the Rb-Sr system closure (4360 Ma):

$$190 \quad \left(\frac{^{87}\text{Sr}}{^{86}\text{Sr}}\right)_{60025}^{T_{FAN}} = \left(\frac{^{87}\text{Sr}}{^{86}\text{Sr}}\right)_{60025}^{\text{today}} - \left(\frac{^{87}\text{Rb}}{^{86}\text{Sr}}\right)_{FAN} (e^{\lambda T_{FAN}} - 1) \quad (1)$$

191 where  $T_{FAN}$  is the age of formation of FAN 60025, and  $\lambda$  is the decay constant of  $^{87}\text{Rb}$  equal to  
 192  $1.3971 \times 10^{-11} \text{ yr}^{-1}$  (Rothenberg et al. 2012). More complex scenarios that we consider unlikely are  
 193 discussed in the Supplement.

194

195 **Table 1.  $^{87}\text{Sr}/^{86}\text{Sr}$  ratios and elemental Rb and Sr concentrations for FAN 60025**

		$^{87}\text{Sr}/^{86}\text{Sr}$	2 s.e.	Rb (ppm)	Sr (ppm)	$^{87}\text{Rb}/^{86}\text{Sr}$
This study	NIST 987 ( $\pm 2$ S.D.)	0.7102487	0.0000004			
	60025 plagioclase*	0.6990809	0.0000011	0.020	196.2	$2.95 \times 10^{-4}$
		0.6990809	0.0000010			
		0.6990817	0.0000013			
		Mean ( $\pm 2$ S.D.)	0.6990812	0.0000009		
Carlson and Lugmair (1988)	60025 plagioclase	0.699102	0.000020	0.0192	196.5	$2.83 \times 10^{-4}$
		0.699090	0.000022			
	60025 mafic minerals	0.699151	0.000040	0.0017	4.976	$9.89 \times 10^{-4}$

196 Data are normalized to  $^{86}\text{Sr}/^{88}\text{Sr} = 0.1194$ . The data of Carlson and Lugmair (1988) was renormalized to the same  
 197 value of the NIST987 standard reported in Table S1. The mass of plagioclase separates used for the three aliquots was  
 198 281.4 mg.

199

## 200 **4. A model for the earliest age of the Moon based on Rb-Sr systematics**

### 201 *4.1 Input parameters*

#### 202 *4.1.1 The initial $^{87}\text{Sr}/^{86}\text{Sr}$ ratio of the Solar System*

203 It has been shown that the nucleosynthetic composition of Sr in planetary materials is not  
 204 identical throughout the Solar System (Hans et al., 2013; Moynier et al., 2012). Most notably,  
 205 carbonaceous chondrites and calcium-aluminium rich inclusions (CAI) show significant anomalies  
 206 expressed as  $\mu^{84}\text{Sr}$  (Charlier et al., 2021; Kleine et al., 2012; Moynier et al., 2012). These  
 207 anomalies were initially attributed to either a p-component excess in  $^{84}\text{Sr}$  or and alternatively it



208 could be due to an r-process component excess in  $^{86}\text{Sr}$  and  $^{88}\text{Sr}$  that would translate to an  $^{84}\text{Sr}$   
209 anomaly after mass fractionation correction using the  $^{86}\text{Sr}/^{88}\text{Sr}$  ratios as is commonly done.  
210 However, Charlier et al. (2021) have argued that it is unlikely to be an r-process component as this  
211 would yield large  $^{87}\text{Sr}$  anomalies in the Allende leachates analyzed in that study. Thus, the  
212 preferred interpretation of Charlier et al. (2021) is that these anomalies are caused by an excess of  
213 p-process nuclide  $^{84}\text{Sr}$ . The presence of these anomalies reveals that the early Solar System was  
214 not fully homogenized with respect to Sr isotopes, unlike what had been argued in earlier studies  
215 (Palme, 2000). This observation for Sr isotopes is fully consistent with other observations made  
216 on refractory elements (Cr, Ti, Mo) that show a clear dichotomy between planetary materials from  
217 the inner solar system (e.g. Trinquier, 2007; Warren 2011; Kleine et al. 2020) and a second  
218 reservoir that could be the outer solar system (i.e. beyond Jupiter). The observed heterogeneity at  
219 the scale of a few astronomical units, indicates that the planetary dust was not well mixed within  
220 the early Solar System.

221  
222 Thus, it has become questionable to use  $^{87}\text{Sr}/^{86}\text{Sr}$  measured in CAI as a reliable initial for  
223 the inner Solar System. One evidence for this comes from measurements in angrites and eucrites,  
224 both classified as non-carbonaceous materials, (e.g., Kleine et al., 2020) that give similar initial  
225  $^{87}\text{Sr}/^{86}\text{Sr}$  ratios (Hans et al. 2013). The initial  $^{87}\text{Sr}/^{86}\text{Sr}$  ratio of angrites and eucrites is difficult to  
226 reconcile with the  $^{87}\text{Sr}/^{86}\text{Sr}$  inferred from CAI, since the nucleosynthetic anomalies in  $^{84}\text{Sr}$  are  
227 solely due to an excess of p-process nuclide. As shown in Hans et al. (2013), if one use the CAI  
228 D7 that has the lowest  $^{87}\text{Sr}/^{86}\text{Sr}$  ratio ever found as the initial Sr isotope ratio of the Solar System  
229 (Papanastassiou and Wasserburg, 1978) to calculate the age of Rb depletion of angrites, it gives  
230 an age of  $7.1\pm 1.6$  Ma, while it yields  $4.6\pm 1.5$  Ma with CAI E38 (note that we used the Rb/Sr ratio  
231 from Barrat et al. (2012) for calculating the Rb depletion age). This means that Rb loss would  
232 postdate the age of accretion of angrites and would correspond to the time when the first crustal  
233 angrite formed. Altogether, these ages are not consistent with those inferred with Hf-W systematics  
234 (Kleine et al., 2012) and with U-Pb and  $^{26}\text{Al}$ - $^{26}\text{Mg}$  systematics (Schiller et al. 2015). It is thus more  
235 reasonable to consider that the initial  $^{87}\text{Sr}/^{86}\text{Sr}$  inferred for angrites and eucrites better represents  
236 the initial ratio of the *inner* solar system, as assumed in recent studies (Mezger et al. 2021 or Borg  
237 et al., 2022) without considering that the CAI could represent the appropriate initial for Sr isotopes.

238 In brief, it is legitimate to use the angrite initial  $^{87}\text{Rb}/^{86}\text{Sr}$  (Hans et al. 2013) as an anchor for the  
239 estimation of the age of the Moon, in what follows.

240

#### 241 4.1.2 Rb/Sr ratio in the bulk silicate Earth and bulk silicate Moon.

242 The  $^{87}\text{Rb}/^{86}\text{Sr}$  ratio of the bulk Silicate Earth (BSE) has been determined in previous studies  
243 (Hofmann and White, 1983; McDonough et al., 1992). For the sake of this study, we redetermined  
244 a new value of the  $^{87}\text{Rb}/^{86}\text{Sr}$  ratio of the bulk silicate Earth using the more recent Ba/Sr ratio  
245 determined in the Orgueil CI chondrite (Barrat et al., 2012). This Ba/Sr value for chondrites (0.318)  
246 is also consistent with the Ba/Sr ratio found in the comprehensive study of Allende (Stracke et al.,  
247 2012; Ba/Sr=0.302) or the study of Barrat et al. (2014) for enstatite chondrites yielding an average  
248 Ba/Sr equal to 0.318 (excluding EL6 which are heavily metamorphosed, Stracke et al., 2012). We  
249 then assume that the Ba/Sr ratio of the BSE is chondritic as both elements are refractory and  
250 lithophile. Since Rb and Ba are both highly incompatible in magmatic processes, it is then possible  
251 to use the constant Rb/Ba ratios measured in terrestrial rocks to infer the  $^{87}\text{Rb}/^{86}\text{Sr}$  ratio of the  
252 BSE:

$$253 \left(\frac{\text{Rb}}{\text{Sr}}\right)_{\text{BSE}} = \left(\frac{\text{Rb}}{\text{Ba}}\right)_{\text{BSE}} \left(\frac{\text{Ba}}{\text{Sr}}\right)_{\text{chondrite}}$$

254 The calculated  $^{87}\text{Rb}/^{86}\text{Sr}$  ratio is equal to 0.079. The  $^{87}\text{Rb}/^{86}\text{Sr}$  value obtained with EH chondrites  
255 is equal to 0.0792, which is marginally different. However, this ratio may not be representative of  
256 the Rb/Sr of the Earth at the time of the Moon formation since this event predates late accretion  
257 (also called late veneer), which is generally assumed to consist of volatile-rich materials. For this  
258 reason, one can also correct the  $^{87}\text{Rb}/^{86}\text{Sr}$  ratio of the bulk Earth for the effect of the late veneer.  
259 The  $^{87}\text{Rb}/^{86}\text{Sr}$  of the Earth prior to the addition of the late veneer is simply inferred by subtracting  
260 a mass fraction of 0.5 % of CI chondrites to the present-day Earth (Day et al., 2007; Walker, 2009).  
261 By subtracting the late veneer contribution, the  $^{87}\text{Rb}/^{86}\text{Sr}$  ratio of the BSE shifts from 0.079 to  
262 0.077. Since CI chondrites represent the most Rb-rich material, this calculation provides a  
263 *minimum* value for the Rb/Sr ratio for the Earth, as long as the percentage of Earth's mass added  
264 by the late veneer does not exceed 0.5%. If the late veneer materials did not consist of CI chondrites  
265 and were depleted in volatile elements compared to CI chondrites (as suggested by Ru isotope  
266 observations, Fisher-Godde et al. 2017), the Rb/Sr ratio of the Earth before the addition of the late  
267 veneer would be comprised between the value calculated above (0.077) and the ratio of the present-

268 day BSE. In the calculations that follow we have considered that the  $^{87}\text{Rb}/^{86}\text{Sr}$  could range between  
269 this minimum value (0.077) and the maximum value taken by Borg et al. (2022) equal to 0.089.  
270 For the bulk Silicate Moon (BSM), a similar approach was used. The mean Rb/Ba ratio estimated  
271 by McDonough et al. (1992) is 0.017, this yields a value of  $^{87}\text{Rb}/^{86}\text{Sr}$  equal to 0.015 for the bulk  
272 silicate Moon. A new estimate of this value was calculated using a compilation of Rb/Ba ratios in  
273 thirty-four lunar rocks using only isotope dilution data (Murthy et al., 1971; Philpotts et al., 1972;  
274 Philpotts and Schnetzler, 1970; Schnetzler and Nava, 1971) and we obtained a value of  
275  $0.0154 \pm 0.0028$  (2 S.D.). This translates into a new estimate of the  $^{87}\text{Rb}/^{86}\text{Sr}$  for the bulk silicate  
276 Moon equal to  $0.0135 \pm 0.0024$  (2 S.D.). Our calculated  $^{87}\text{Rb}/^{86}\text{Sr}$  for the BSM is significantly lower  
277 than the  $^{87}\text{Rb}/^{86}\text{Sr}$  suggested in previous publications for FAN 60025 (e.g., Carlson et al. 2014;  
278 Carlson and Lugmair, 1988). However, in order to be conservative, we have considered in our  
279 calculations a broader range from  $2.7 \times 10^{-4}$  (assuming it is equal to the Rb/Sr of FAN) to 0.022.

280

#### 281 *4.2 Determination of the age of the Moon*

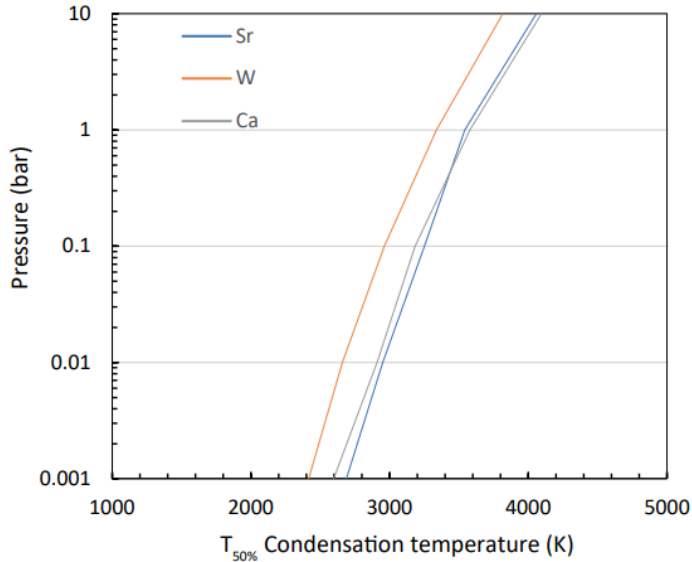
282

283 A striking observation is the similarity in the isotope composition of refractory elements in the  
284 Moon and Earth such as Si, Ca, Mg, Cr, Ti, O (Armytage et al., 2012; Fitoussi and Bourdon, 2012;  
285 Mougél et al., 2018; Schiller et al., 2018; Sedaghatpour et al., 2013; Young et al., 2016; Zhang et  
286 al., 2012). Understanding these observations has been a challenging task over the years. The quasi-  
287 coincidence in isotope signatures between Moon and Earth had initially been used to infer that the  
288 Moon and the bulk silicate Earth have equilibrated with each other at the time of the impact  
289 (Armytage et al., 2012; Fitoussi and Bourdon, 2012; Young et al., 2016). A mean of alleviating  
290 this constraint could be that Theia and the proto-Earth contributed to equal proportions in the Moon  
291 and the Earth resulting in homogeneous isotope composition (Canup 2012). As an alternative,  
292 Dauphas et al. (2014) have hypothesized that the Earth and Theia came from similar regions in the  
293 inner Solar System and had in fact similar O, Cr and Ti isotope compositions. This interpretation  
294 would no longer require an equilibration process as described in various studies (Lock et al., 2018;  
295 Lock and Stewart, 2017; Pahlevan and Stevenson, 2007). Borg et al. (2022) went further by stating  
296 that this hypothesis was also consistent with Rb/Sr ratios lower than that of chondrites, both in  
297 Theia and the proto-Earth, indicating a global volatile element depletion that pre-dated the Giant  
298 Impact. However, this interpretation conflicts with the Hf-W (Kruijjer and Kleine 2017; Fischer et

299 al. 2021) and Si isotope evidence (Armytage et al., 2012; Fitoussi and Bourdon, 2012). Since Theia  
300 and the proto-Earth were unlikely to have had the same evolution in terms of core formation (Hf/W  
301 ratio and age of core formation), it is very unlikely that they had similar  $^{182}\text{W}$  abundances in their  
302 silicate mantles. This was even shown quantitatively by Kruijer and Kleine (2017) who  
303 demonstrated that the probability that Moon and Earth initially shared the same  $\epsilon^{182}\text{W}$  is less than  
304 5%. Thus, in other words, the similarity in  $^{182}\text{W}/^{184}\text{W}$  ratios for Earth and Moon is not just a  
305 coincidence, it must have resulted from a homogeneization process following the giant impact.  
306 A similar argument can be made based on Si, Ca, Mg and Fe stable isotope signatures (e.g.,  
307 Armytage et al., 2012; Fitoussi and Bourdon, 2012; Fu et al. 2023). The Si isotope data show  
308 identical  $\delta^{30}\text{Si}$  in the Moon and the BSE, while they are distinct from all other planetary materials.  
309 Si isotopes can be affected by the processes of planetary accretion (Hin et al., 2017; Kadlag et al.  
310 2021) and core differentiation (Hin et al., 2014; Shahar et al. 2011). There is no particular reason  
311 to believe that Theia would have inherited the same  $\delta^{30}\text{Si}$  as the proto-Earth, even though it might  
312 have carried the same nucleosynthetic anomalies. Thus, if the Moon consisted mainly of material  
313 derived from Theia as argued in Borg et al. (2022), it would have inherited a silicon isotope  
314 signature distinct from that of the Earth. Fu et al. (2023) further emphasized that in the context of  
315 the traditional impact models, one does not expect an equilibration between BSE and BSM simply  
316 because the Moon stems mostly from the Theia and the energy associated with the impact is  
317 insufficient to produce thorough mixing. This is another argument for an isotope equilibration  
318 between the Moon and the bulk silicate Earth following the giant impact. As an additional  
319 argument, we have calculated the condensation temperatures of Sr, Ca and W in the conditions of  
320 the Moon formation. The results (Figure 1) show that Sr was volatile in the early stages of the  
321 proto-lunar disk evolution and that its volatility is similar to that of Ca and W. Thus, this is a direct  
322 new argument for Sr isotope equilibration, since there is direct evidence for equilibration of Ca  
323 and W isotopes between Moon and Earth, this must be the case for Sr as well.

324

325



326

327 **Figure 1**

328 Condensation temperature (50%) for Ca, Sr and W calculated using the approach described in  
 329 Ivanov et al. (2022) as a function of pressure as described in the Supplementary materials. The  
 330 results show that Sr is of similar volatility to Ca and W, which are both elements that have  
 331 equilibrated isotopically between the Moon and bulk silicate Earth, following the Moon forming  
 332 impact.

333

334

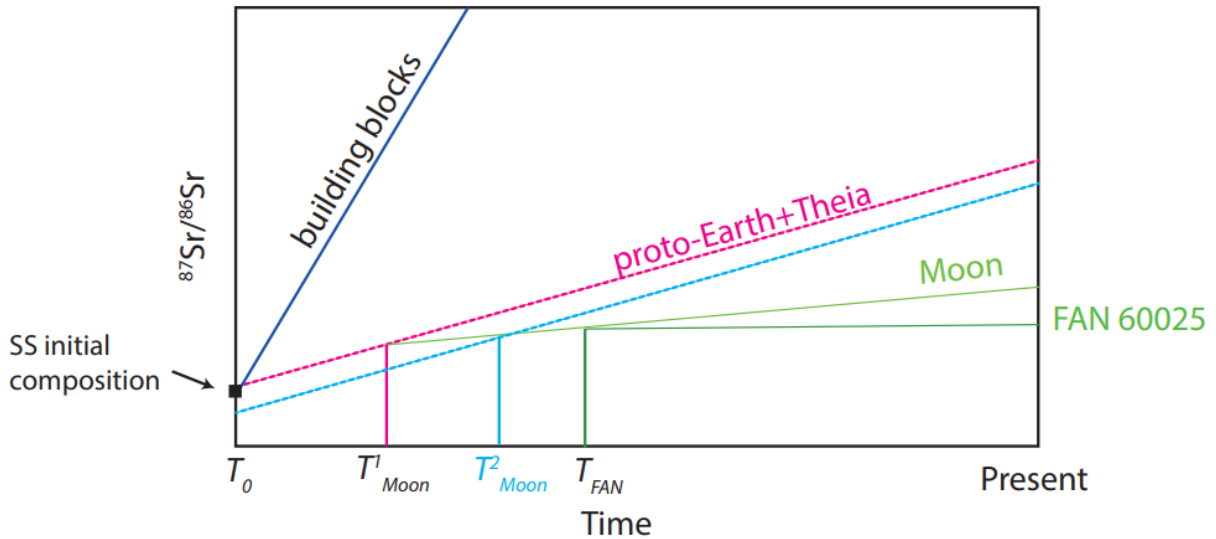
335 In this study, similarly to Halliday (2008) and Mezger et al. (2021), we have considered that the  
 336 proto-Earth and Theia have equilibrated and therefore considered that the  $^{87}\text{Sr}/^{86}\text{Sr}$  of the Moon  
 337 and the Earth were identical at the time of the Moon-forming impact due to efficient mixing, which  
 338 is consistent with a high energy structure, as that described in Lock et al. (2018). Reaching such a  
 339 high energy structure stems directly from the models of Cuk and Stewart (2012) or Canup (2012),  
 340 where the final thermal structure of the proto-lunar disk or synestia directly depends on the  
 341 parameters of the collision between proto-Earth and Theia (e.g. Nakajima et al. 2014).

342

343 With this hypothesis, it is possible to determine the  $^{87}\text{Sr}/^{86}\text{Sr}$  ratio of the Bulk Silicate Moon as a  
 344 function of the time of Moon formation (see details below). By further assuming that the proto-  
 345 Earth started evolving at  $T_0$  with an  $^{87}\text{Rb}/^{86}\text{Sr}$  equal to that of the BSE+Moon system, it is then  
 346 possible to calculate the age of the Moon by stating that at that time, the  $^{87}\text{Sr}/^{86}\text{Sr}$  ratio in Moon

347 and Earth were equal (See Figure 2). As shown in Figure 2, if  $T_{\text{Moon}}$  is shifted to a younger value,  
 348 this requires that the initial  $^{87}\text{Sr}/^{86}\text{Sr}$  ratio of the inner Solar System has to be below the observed  
 349 value. Thus, the calculated age corresponds to the youngest possible age for the Moon. In what  
 350 follows, this approach is explained in more details.

351



352

353

354 **Figure 2.** Schematic view of the  $^{87}\text{Sr}/^{86}\text{Sr}$  temporal evolution for the bulk system (Proto-  
 355 Earth+Theia) and the Moon illustrating the principle used for calculating the youngest age of the  
 356 Moon. The initial  $^{87}\text{Sr}/^{86}\text{Sr}$  of FAN 60025 is calculated at 4.360 Ga (dark green line). This ratio is  
 357 then used to calculate the  $^{87}\text{Sr}/^{86}\text{Sr}$  of the Moon at  $T^1_{\text{Moon}}$  the age of its formation (light green line).  
 358 Assuming that the bulk system evolved from initial  $^{87}\text{Sr}/^{86}\text{Sr}$  of the Solar System ‘SS’ at  $T_0 = 4.567$   
 359 Ga to a common composition at  $T^1_{\text{Moon}}$ , it is possible to calculate the age that matches this  
 360 constraint (intersect of red and light green lines). If the age of Moon formation is shifted to a  
 361 younger age  $T^2_{\text{Moon}}$ , the initial  $^{87}\text{Sr}/^{86}\text{Sr}$  of the Solar System has to be below the observed value.  
 362 This defines a youngest age for the Moon.

363

364 If one assumes that the initial  $^{87}\text{Sr}/^{86}\text{Sr}$  ratio in the inner Solar System is indeed that defined based  
 365 on angrites and eucrites (Hans et al. 2013; Mezger et al. 2021; Borg et al. 2022), it is possible to  
 366 estimate the  $^{87}\text{Sr}/^{86}\text{Sr}$  of the bulk system (proto-Earth+Theia) by assuming that it evolved as a  
 367 closed system until the Moon formed (Figure 2).

368 
$$\left(\frac{^{87}\text{Sr}}{^{86}\text{Sr}}\right)_{E+M}^{T_{\text{Moon}}} = \left(\frac{^{87}\text{Sr}}{^{86}\text{Sr}}\right)_{E+M}^{T_0} + \left(\frac{^{87}\text{Rb}}{^{86}\text{Sr}}\right)_{E+M} (e^{\lambda T_0} - e^{\lambda T_{\text{Moon}}}) \quad (2)$$

369 where E+M designates the bulk system (Earth+Moon),  $T_0$ , the age of the beginning of the Solar  
 370 System as defined by CAI and  $T_{\text{Moon}}$  is the age of Moon formation. The bulk system consists of  
 371 the proto-Earth and Theia, both of which have an unknown composition. However, if we assume  
 372 mass conservation, then the composition of the bulk system is equal to the composition of the  
 373 Earth+Moon system. In recent models for the Moon formation, the volatile elements that may have  
 374 been lost from the Moon are reaccreted onto the Earth (Charnoz and Michaut 2015; Lock et al.  
 375 2018; Charnoz et al. 2021). The  $^{87}\text{Rb}/^{86}\text{Sr}$  of the bulk system can thus be calculated as:

376 
$$\frac{^{87}\text{Rb}}{^{86}\text{Sr}}_{E+M} = \frac{^{87}\text{Rb}}{^{86}\text{Sr}}_{BSE} X_{BSE}^{\text{Sr}} + \frac{^{87}\text{Rb}}{^{86}\text{Sr}}_{BSM} (1 - X_{BSE}^{\text{Sr}})$$

377 where  $X_{BSE}^{\text{Sr}}$  is the mass fraction of  $^{86}\text{Sr}$  from the bulk silicate Earth in the E+M system (=0.982)  
 378 assuming a lunar core representing 1% of the lunar mass. If we then assume that the Moon and the  
 379 Earth had identical  $^{87}\text{Sr}/^{86}\text{Sr}$  ratios at the time of the giant impact, it is possible to estimate the age  
 380 of the Moon-forming impact by calculating the time at which the compositions of the bulk system  
 381  $^{87}\text{Sr}/^{86}\text{Sr}$  and of the Moon  $^{87}\text{Sr}/^{86}\text{Sr}$  coincided, as shown in an  $^{87}\text{Sr}/^{86}\text{Sr}$  (t) versus time diagram  
 382 (Figure 2). The intersection of evolution line of the bulk system and that of the bulk silicate Moon  
 383 composition defines the age of the Moon (Figure 2). The parameters used for this calculation are  
 384 given in Table S3. The assumption that the Earth and the Moon had similar Sr isotope compositions  
 385 at the time the Moon formed is written as:

386 
$$\left(\frac{^{87}\text{Sr}}{^{86}\text{Sr}}\right)_{\text{Moon}}^{T_{\text{Moon}}} = \left(\frac{^{87}\text{Sr}}{^{86}\text{Sr}}\right)_{E+M}^{T_{\text{Moon}}} \quad (3)$$

387 Fortunately, it is also possible to determine independently the  $^{87}\text{Sr}/^{86}\text{Sr}$  ratio of the bulk silicate  
 388 Moon at the time of Moon formation,  $T_{\text{Moon}}$  based on lunar rock data. The revised crystallization  
 389 age for FAN 60025 equal to  $4.360 \pm 0.003$  Ga obtained by Borg et al. (2011) implies that the initial  
 390  $^{87}\text{Sr}/^{86}\text{Sr}$  ratio of FAN 60025 cannot be taken as representative of the Moon initial  $^{87}\text{Sr}/^{86}\text{Sr}$  ratio  
 391 as assumed in Halliday (2008) and Halliday and Porcelli, (2001), unless the age of anorthosite is  
 392 equal to the age of Moon. This is an important difference with these previous studies. Anorthosites  
 393 such as FAN 60025 are thought to have formed in the last 70-80% of the lunar magma ocean  
 394 crystallization by plagioclase flotation. Based on their history, it is possible to consider two  
 395 possibilities. As a first possibility (Model A, Figure S1), one can assume that the mantle source of

396 anorthosites is similar to that of the bulk silicate Moon with an  $^{87}\text{Rb}/^{86}\text{Sr}=0.014\text{-}0.019$  (Halliday  
 397 and Porcelli, 2001; Ringwood and Kesson, 1977; Borg et al. 2022) (Model A, see Figure S1). This  
 398 makes the implicit assumption that the preceding stages of the lunar magma ocean crystallization  
 399 induced little variation in the Rb/Sr ratio. Given that phases crystallizing prior to anorthosite have  
 400 been shown to be olivine and orthopyroxene (Elardo et al., 2011; Elkins-Tanton et al., 2011), this  
 401 is a reasonable assumption because these phases should not greatly fractionate the Rb/Sr ratio. A  
 402 second possibility (Model B) is to assume that the mantle reservoir producing the FAN was as  
 403 depleted in Rb as the anorthosite itself (Model B,  $\text{Rb}/\text{Sr}_{\text{FAN}}=\text{Rb}/\text{Sr}_{\text{BSM}}$ , see Figure S1) since the  
 404 time of Moon formation. This second option implicitly assumes that the anorthosite reservoir  
 405 would have formed rapidly after lunar accretion, a hypothesis that would imply a rapid  
 406 crystallization of the magma ocean (Elkins-Tanton et al., 2011) and that this reservoir evolved as  
 407 a closed system until formation of the anorthosite itself. In this case, the late Sm-Nd and U-Pb age  
 408 of FAN 60025 could be attributed to thermal resetting or remelting of existing anorthosite-rich  
 409 material.

410 We first consider that the Sr isotope composition of 60025 was that of the bulk silicate Moon  
 411 between the time of Moon formation until the time of the anorthosite formation  $T_{\text{FAN}}$ , (Model A)  
 412 and using a standard equation for radioactive decay in a closed system, the  $^{87}\text{Sr}/^{86}\text{Sr}$  ratio for the  
 413 Moon when the Moon formed can be deduced from the following equation:

$$414 \quad \left(\frac{^{87}\text{Sr}}{^{86}\text{Sr}}\right)_{60025}^{T_{\text{FAN}}} = \left(\frac{^{87}\text{Sr}}{^{86}\text{Sr}}\right)_{\text{Moon}}^{T_{\text{Moon}}} + \left(\frac{^{87}\text{Rb}}{^{86}\text{Sr}}\right)_{\text{BSM}} (e^{\lambda T_{\text{Moon}}} - e^{\lambda T_{\text{FAN}}}) \quad (4)$$

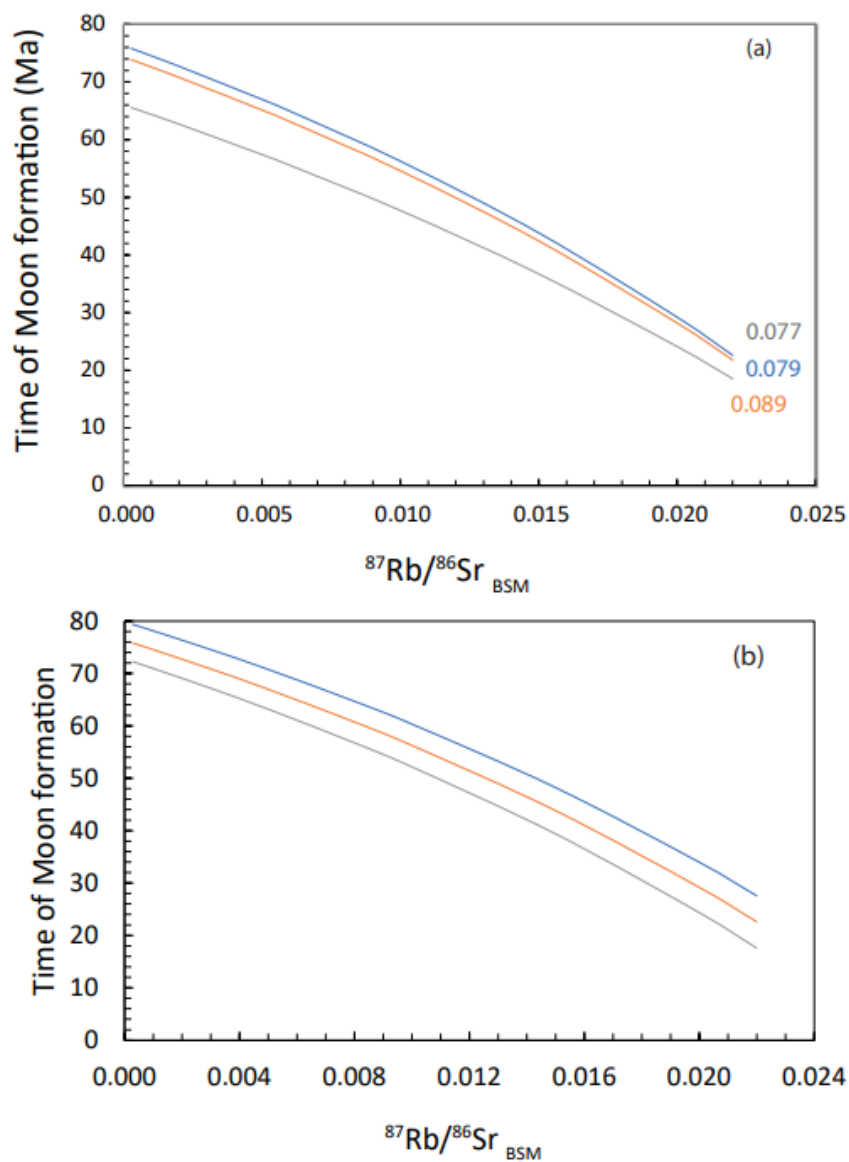
415 where  $T_{\text{FAN}}$  is the age of formation of the ferro-anorthosite. Alternatively, in the case of Model B,  
 416 we can also assume that the  $^{87}\text{Rb}/^{86}\text{Sr}$  of this sample is equal to that of FAN 60025 rather than that  
 417 of the BSM from  $T_{\text{Moon}}$  to  $T_{\text{FAN}}$ . The Sr isotope composition of FAN 60025 at the time of its  
 418 formation  $T_{\text{FAN}}$  can be deduced from the measured value (Table S2) using equation (4) shown  
 419 above. Combining equations (1)-(4), it is then possible to calculate the age of the Moon:

$$420 \quad T_{\text{Moon}} = \frac{1}{\lambda} \ln \left( \frac{\left(\frac{^{87}\text{Sr}}{^{86}\text{Sr}}\right)_{60025}^{\text{today}} - \left(\frac{^{87}\text{Rb}}{^{86}\text{Sr}}\right)_{\text{FAN}} (e^{\lambda T_{\text{FAN}}} - 1) - \left(\frac{^{87}\text{Sr}}{^{86}\text{Sr}}\right)_{\text{E+M}}^{T_0} + \left(\frac{^{87}\text{Rb}}{^{86}\text{Sr}}\right)_{\text{BSM}} e^{\lambda T_{\text{FAN}}} - \left(\frac{^{87}\text{Rb}}{^{86}\text{Sr}}\right)_{\text{E+M}} e^{\lambda T_0}}{\left(\frac{^{87}\text{Rb}}{^{86}\text{Sr}}\right)_{\text{BSM}} - \left(\frac{^{87}\text{Rb}}{^{86}\text{Sr}}\right)_{\text{E+M}}} \right) \quad (5)$$

422 The equation for Model B is identical, except that we replace  $\left(\frac{^{87}\text{Rb}}{^{86}\text{Sr}}\right)_{\text{BSM}}$  by  $\left(\frac{^{87}\text{Rb}}{^{86}\text{Sr}}\right)_{\text{FAN}}$ .



423 The age of the Moon was calculated using equation (5) and the results are plotted in Figures 3 and  
 424 4 for various values of the input parameters. In these calculations, the most sensitive parameter is  
 425 the  $^{87}\text{Rb}/^{86}\text{Sr}$  of the bulk Silicate Moon, which is used as the x-axis for plotting the results.  
 426

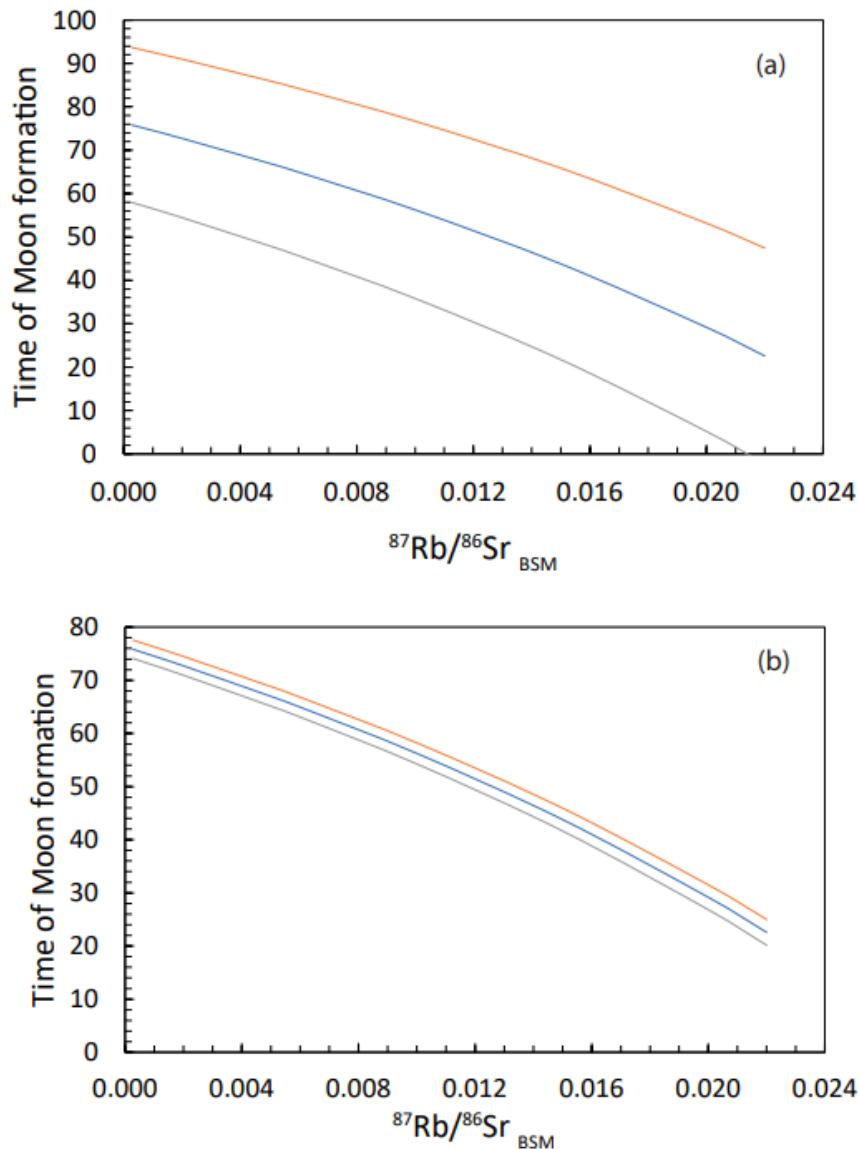


427  
 428  
 429 **Figure 3** (a) Forward model for the calculation of the age of the Moon based on Rb-Sr isotope  
 430 systematics showing the sensitivity of the age determination to  $^{87}\text{Rb}/^{86}\text{Sr}$  ratio of the bulk Silicate  
 431 Moon (BSM) and to the uncertainty to the  $^{87}\text{Rb}/^{86}\text{Sr}$  ratio of the Bulk Silicate Earth with the values  
 432 labeled on the curves. (b) Forward model for the calculation of the age of the Moon based on Rb-

433 Sr isotope systematics showing the sensitivity of the age determination to  $^{87}\text{Rb}/^{86}\text{Sr}$  ratio of the  
434 bulk Silicate Moon (BSM) and to the uncertainty on the initial  $^{87}\text{Sr}/^{86}\text{Sr}$  ratio of the inner Solar  
435 System (Hans et al. 2013). The blue curve corresponds to the mean value  $\mu=0.698978$ , while the  
436 yellow and grey curves corresponds to  $\mu+2\sigma$  and  $\mu-2\sigma$ , respectively with  $2\sigma=0.000004$ .

437  
438 If we assume that Model A is correct, the age of the Moon is equal to 45 Ma for an  $^{87}\text{Rb}/^{86}\text{Sr}$  ratio  
439 in the BSE equal to 0.079. If we now assume that Model B is correct, then the age of the Moon is  
440  $73.9 \pm 0.8$  Ma for an  $^{87}\text{Rb}/^{86}\text{Sr}$  ratio in the BSE equal to 0.079 (the quoted uncertainty takes only  
441 into account the uncertainty on the measurements of FAN 60025, corresponding to fixed  $^{87}\text{Rb}/^{86}\text{Sr}$   
442 values in the BSM and BSE. For the sake of comparison, if one uses the analytical uncertainties  
443 on the measured  $^{87}\text{Sr}/^{86}\text{Sr}$  ratio for FAN 60025, reported by Carlson and Lugmair (1988), with the  
444 same values of  $^{87}\text{Rb}/^{86}\text{Sr}$  ratios in the Moon and Earth, then the maximum age of the Moon would  
445 range between 24.7 and 68.2 Ma with Model A and between 58.0 and 93.7 Ma with Model B  
446 (Figure 4). Thus, the improvement in analytical uncertainty of FAN 60025 is critical for improving  
447 the age uncertainty (see also below for a detailed assessment).

448



449  
 450 **Figure 4** Forward model for the calculation of the age of the Moon based on Rb-Sr isotope  
 451 systematics showing the sensitivity of the age determination to the initial  $^{87}\text{Sr}/^{86}\text{Sr}$  ratio of the  
 452 ferro-anorthosite 60025 (a) uncertainties are those reported in Carlson and Lugmair (1988) which  
 453 is approximately 28 ppm. (b) uncertainties are those reported in Table S2, this study. There is a  
 454 clear reduction of uncertainty on the age determination based on the new data.

455

456

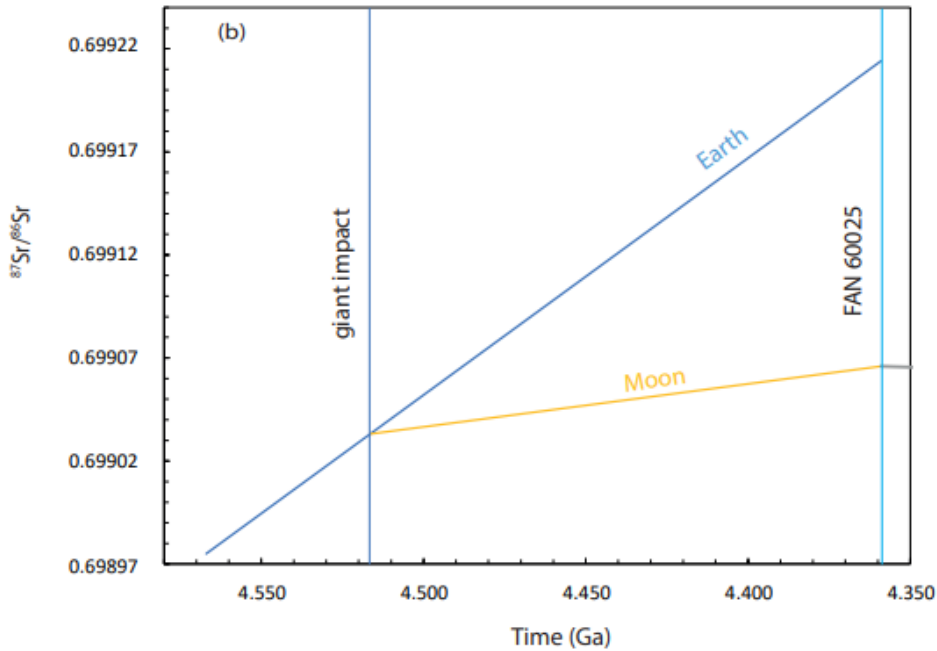
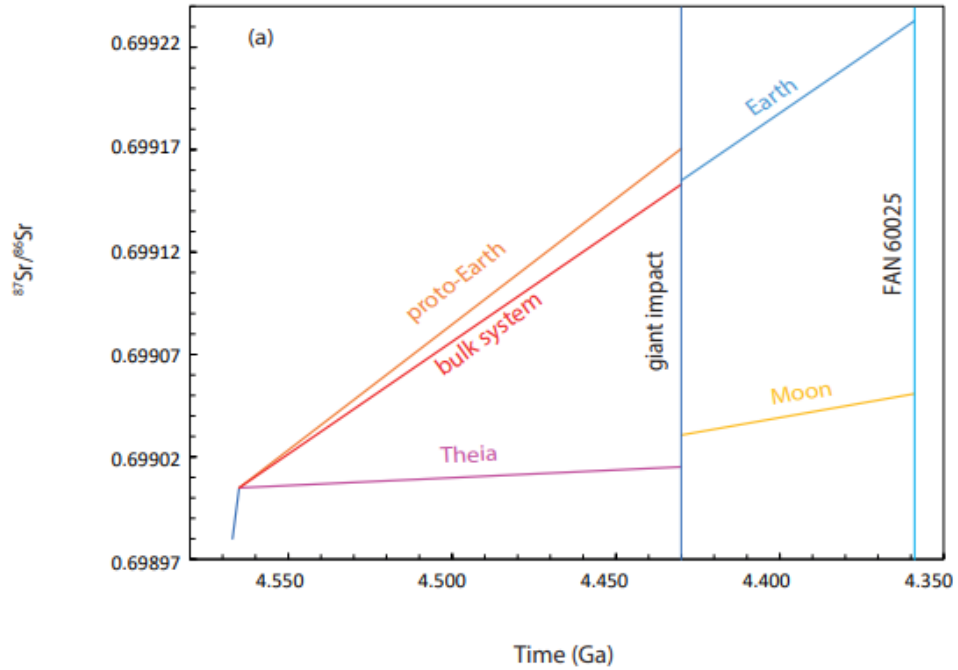
457 A further refinement is that one can consider the existence of late accretion that could have  
 458 modified the Rb/Sr ratio of the BSE and this late accretion was not identical for Moon and Earth

459 (Kruijer et al., 2015; Touboul et al., 2015). If we subtract the contribution of late accreted material  
460 to the BSE assuming that this contribution consisted of chondrites, then the estimated age of the  
461 Moon becomes 46.4 Ma instead of 45.0 Ma (Model A). This indicates that if we combine the  
462 results obtained from Model A and B, the youngest possible age of the Moon is 79.4 Ma after the  
463 beginning of the Solar System. In Figures 3 and 4, we have investigated the sensitivity of the Moon  
464 age on possible input parameters, namely  $^{87}\text{Rb}/^{86}\text{Sr}$  of BSE,  $^{87}\text{Rb}/^{86}\text{Sr}$  of BSM, initial  $^{87}\text{Sr}/^{86}\text{Sr}$  of  
465 the Solar System, initial  $^{87}\text{Sr}/^{86}\text{Sr}$  of FAN 60025. One of the most sensitive parameters is the  
466  $^{87}\text{Rb}/^{86}\text{Sr}_{\text{BSM}}$ ; as shown in Figure 3-4, the youngest age (79.4 Ma) is obtained for a low  $^{87}\text{Rb}/^{86}\text{Sr}$   
467 in the BSM while an older age (17.6 Ma) corresponds to the highest  $^{87}\text{Rb}/^{86}\text{Sr}_{\text{BSM}}$  value (0.022).  
468 As mentioned above, the calculated age is also very sensitive to the uncertainty on the initial  
469  $^{87}\text{Sr}/^{86}\text{Sr}$  of FAN 60025. If one takes the uncertainty of 28 ppm on  $^{87}\text{Sr}/^{86}\text{Sr}$  reported in Carlson  
470 and Lugmair (1988) then the youngest age becomes 94 Ma with the lowest bound being 0 Ma  
471 (Figure 4a). In contrast, if one uses the newly determined  $^{87}\text{Sr}/^{86}\text{Sr}$  with an uncertainty of 2.4 ppm,  
472 then this range becomes 75.8-79.4 Ma (Figure 4b). The least sensitive parameter is  $^{87}\text{Rb}/^{86}\text{Sr}_{\text{BSE}}$ ,  
473 given a reasonable range of input values from 0.077 to 0.089 as shown in Figure 3. Similarly, the  
474 uncertainty on the initial  $^{87}\text{Sr}/^{86}\text{Sr}$  of inner Solar System also has a limited impact on the calculated  
475 Moon age (Figure 3b).

476

477

478



479

480 **Figure 5**

481  $^{87}\text{Sr}/^{86}\text{Sr}$  versus time diagram to illustrate the differences between (a) the model of Borg et al.  
 482 (2022) and (b) the model presented in this study. The model of Borg et al. (2022) shown here was  
 483 redrawn based on the parameters given in their Table S1 (Model 6). During the first stage, the  
 484 system evolves as a closed system with  $^{87}\text{Rb}/^{86}\text{Sr} = 0.832$  (CI chondrites). After 2 Ma, proto-Earth

485 and Theia form and evolve as closed systems until the time of the impact. The time evolution of  
486 the bulk system (Theia + proto-Earth) was recalculated and is shown as a red line. Note that it is  
487 very similar to the evolution of the BSE after the impact. This model clearly shows that the  
488 composition of the bulk silicate Earth is more radiogenic than that of the Moon, which consists  
489 mainly of Theia. The time of the impact is fixed arbitrarily to match the composition of the Moon  
490 using plausible mixing proportions. (b) in this study, the  $^{87}\text{Sr}/^{86}\text{Sr}$  of the bulk system (recalculated  
491 based on the Moon + BSE mass balance) evolves as a closed system, until the time of the impact  
492 when Earth and Moon equilibrated isotopically. The time of the impact is fixed such that the  
493  $^{87}\text{Sr}/^{86}\text{Sr}$  ratio of the Moon is equal to that of the bulk system.

494

495 Our results clearly differ from those of Borg et al. (2022) and for the sake of clarity, we have  
496 reproduced their calculations using their model 6 (Table S1 in Borg et al. 2022). The results are  
497 plotted in Figure 5a and directly compared with one of our models (Figure 5b) using the same  
498 scale in X and Y. The obvious difference is that they do not assume that Earth and Moon had  
499 similar  $^{87}\text{Sr}/^{86}\text{Sr}$  due to isotope equilibration after the giant impact, hence the  $^{87}\text{Sr}/^{86}\text{Sr}$  of the post  
500 impact Earth is significantly more radiogenic than that of the Moon. We have calculated in addition  
501 the  $^{87}\text{Rb}/^{86}\text{Sr}$  ratio of the bulk system and it is in fact very close to that of the bulk silicate Earth  
502 after the impact. This diagram also illustrates the closed system evolution of Theia and proto-Earth  
503 in the stage preceding the impact with a Rb loss taking place 2 Ma after the beginning of the Solar  
504 System. In what follows, we propose a model where the Rb loss is not necessarily linked with a  
505 unique event of Rb loss, which is strongly restrictive.

506

## 507 **5. MonteCarlo simulations of the age of Moon formation.**

508 The model presented in the previous sections illustrates conceptually the method for  
509 calculating the age of the Moon but it is not fully satisfactory from a conceptual viewpoint. In the  
510 previous scenario (similarly to all published models), we have made some simple assumptions  
511 about the  $^{87}\text{Rb}/^{86}\text{Sr}$  evolution of the system by stating that proto-Earth+Theia system had the  
512  $^{87}\text{Rb}/^{86}\text{Sr}$  ratio of the BSE (+Moon) since the beginning of the Solar System and that it remained  
513 a closed system since then. However, this scenario is rather restrictive. By essence, the accretion  
514 process does not fulfil the conditions of a closed system and it is known that planetary bodies of  
515 the inner Solar System do not share a common  $^{87}\text{Rb}/^{86}\text{Sr}$  value, with values ranging between that

516 of angrites ( $5 \times 10^{-3}$ ) up to the maximum  $^{87}\text{Rb}/^{86}\text{Sr}$  found in CI chondrites (0.8-0.9). Thus, it is more  
 517 realistic to consider a model where the  $^{87}\text{Rb}/^{86}\text{Sr}$  of the accreting Earth constantly evolves due to  
 518 contribution of bodies with variable Rb-Sr history.

519 In what follows, we describe a MonteCarlo approach that includes all sources of uncertainties and  
 520 considers a more realistic Rb-Sr evolution prior to the Moon formation. The evolution starting  
 521 from the beginning of the Solar System is described by N steps of equal duration ( $\Delta t$ ) until the  
 522 time of Moon formation ( $T_{\text{Moon}}$ ). At each step, a fraction of Sr,  $f_{\text{Sr}}^i$  is added to the growing Earth  
 523 whose initial mass of Sr is assumed to be  $M_0$ . The new  $^{87}\text{Sr}/^{86}\text{Sr}$  at step i is thus:

$$524 \quad \frac{^{87}\text{Sr}}{^{86}\text{Sr}}_{\text{init}} = f_{\text{Sr}}^i \frac{^{87}\text{Sr}}{^{86}\text{Sr}}_{i-1} + (1 - f_{\text{Sr}}^i) \frac{^{87}\text{Sr}}{^{86}\text{Sr}}_{\text{in}}$$

525 A similar equation can be written for  $^{87}\text{Rb}/^{86}\text{Sr}$ . At each time step, an object with a random mass  
 526 was accreted and the  $^{87}\text{Rb}-^{87}\text{Sr}$  characteristics of this object were determined according to the  
 527 following rules: the  $^{87}\text{Sr}/^{86}\text{Sr}$  ratio of accreted objects was assumed to evolve starting from the  
 528 initial of the Solar System defined by angrites, until it is accreted with an  $^{87}\text{Rb}/^{86}\text{Sr}$  ratio that is  
 529 allowed to take a random value between 0 ( $\approx$ angrites) and 0.832 (CI chondrites). In addition, the  
 530 accretionary process could randomly lower this ratio upon accretion, mimicking the effect of  
 531 volatile element depletion after a giant impact or any other thermal process. Although this process  
 532 is not well constrained, the volatile loss could be due to the impact itself or to the generation of a  
 533 magma ocean that would lose its volatile (e.g. Hin et al., 2017). A decay equation is then used to  
 534 calculate the in-grown  $^{87}\text{Sr}$ :

$$535 \quad \frac{^{87}\text{Sr}}{^{86}\text{Sr}}_i = f_{\text{Sr}}^i \frac{^{87}\text{Sr}}{^{86}\text{Sr}}_{i-1} + (1 - f_{\text{Sr}}^i) \frac{^{87}\text{Sr}}{^{86}\text{Sr}}_{\text{in}} + k_{\text{Rb}} \frac{^{87}\text{Rb}}{^{86}\text{Sr}} (e^{\lambda T_{i-1}} - e^{\lambda T_i})$$

536 The proto-Earth, is then assumed to grow until it reaches a mass fraction of Sr equal to 1  
 537 corresponding to a full accretion. The parameter  $f_{\text{Sr}}^i$  represents the mass fraction of Sr added at  
 538 each time step and  $k_{\text{Rb}}$  is a coefficient ranging between 0 and 1 representing a random Rb loss  
 539 linked with accretion. Since Sr is a refractory element, we assume that its concentration is constant  
 540 in the accreted material. In this case, the differential equation describing the evolution of  $^{87}\text{Sr}/^{86}\text{Sr}$   
 541 in the silicate mantle can be written as:

$$542 \quad \frac{d \ ^{87}\text{Sr}/^{86}\text{Sr}}{dt} = \frac{1}{M} \frac{dM}{dt} \left[ \frac{C_{\text{me}}^{87}}{C_{\text{me}}^{86}} \frac{C_{\text{me}}^{86}}{C_{\text{m}}^{86}} - \frac{C_{\text{m}}^{87}}{C_{\text{m}}^{86}} \right] - \frac{C_{\text{m}}^{87}}{C_{\text{m}}^{86}} \left[ \frac{C_{\text{me}}^{86}}{C_{\text{m}}^{86}} - 1 \right]$$

543 where the subscripts m and me represent the mantle of Earth and the mantle of accreted material,  
 544 respectively and  $C_k^i$  denotes the concentration of isotope i in reservoir k (i.e. me or m). Since  $C_{me}^{86} =$   
 545  $C_m^{86}$ , the above equation can be simplified to:

$$546 \quad \frac{d \text{}^{87}\text{Sr}/\text{}^{86}\text{Sr}}{dt} = \frac{1}{M} \frac{dM}{dt} \left[ \frac{C_{me}^{87}}{C_{me}^{86}} - \frac{C_m^{87}}{C_m^{86}} \right]$$

547 If this equation is discretized over a time step  $\Delta t$ ; it becomes:

$$548 \quad \frac{\text{}^{87}\text{Sr}_i}{\text{}^{86}\text{Sr}_i} - \frac{\text{}^{87}\text{Sr}_{i-1}}{\text{}^{86}\text{Sr}_{i-1}} = \frac{1}{M} \frac{dM}{dt} \Delta t \left[ \frac{\text{}^{87}\text{Sr}_{me}}{\text{}^{86}\text{Sr}_{me}} - \frac{\text{}^{87}\text{Sr}_{i-1}}{\text{}^{86}\text{Sr}_{i-1}} \right]$$

549 In this expression, one can recognize that:

$$550 \quad f_{Sr} = \frac{1}{M} \frac{dM}{dt} \Delta t$$

551 If this equation is discretized, the accreted mass at time  $i\Delta t$  can be calculated as a function of  $f_{Sr}^i$   
 552 defined at step i:

$$553 \quad f_{Sr}^i = \frac{1}{M_i} (M_i - M_{i-1}) = \frac{\Delta M_i}{M_i}$$

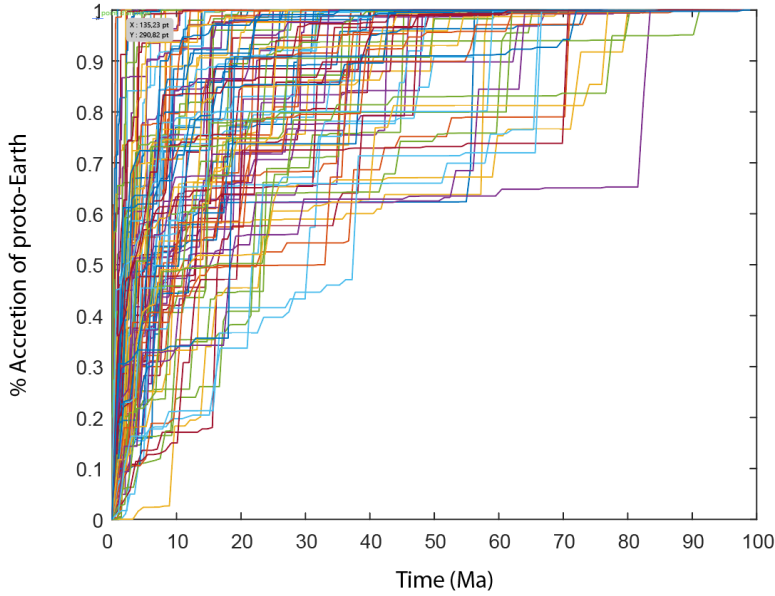
554 In other words,  $f_{Sr}^i$  represent a relative incremental mass accreted at time step i. The accretion of  
 555 the proto-Earth was assumed to take place over N time steps (N=120) until the Earth reached its  
 556 present mass. If we assume that the size of  $M_0$  can vary between a 1 km to 1000 km object, then a  
 557 large range of growth curves can be constructed (Figure 6). In order to generate growth curves that  
 558 are similar to the growth curves of planetary embryos (e.g., Thommes et al., 2003), we used the  
 559 following function for the accreted mass:

$$560 \quad \Delta M_i = rand^i$$

561 where rand is a random number between 0 and 1 and i represents the time step. For each trial, a  
 562 new random value of  $f_{Sr}^i$  is calculated at each time step.

563





564

565 **Figure 6** Sample of random growth curves for the Earth generated in the MonteCarlo simulations  
 566 mimicking typical accretion curves produced in numerical simulations (e.g., Thommes et al. 2003)  
 567 A value of 1 indicates 100% accretion.

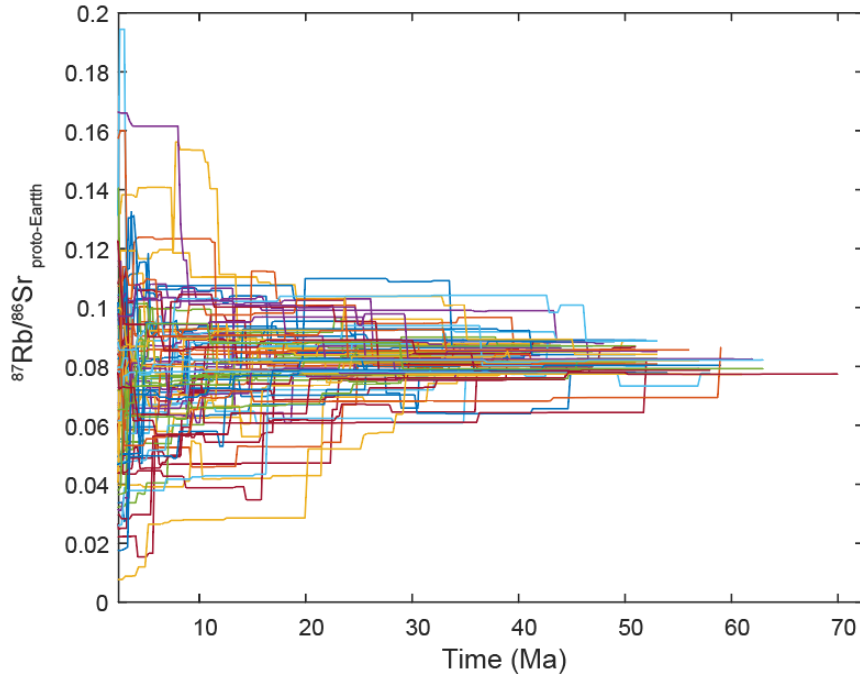
568

569

570 Table S2 shows the range of a priori input parameters used in the MonteCarlo simulation. Figure  
 571 7 shows examples of  $^{87}\text{Rb}/^{86}\text{Sr}$  evolution in the proto-Earth as a function of time for various  
 572 simulations.

573

574



575

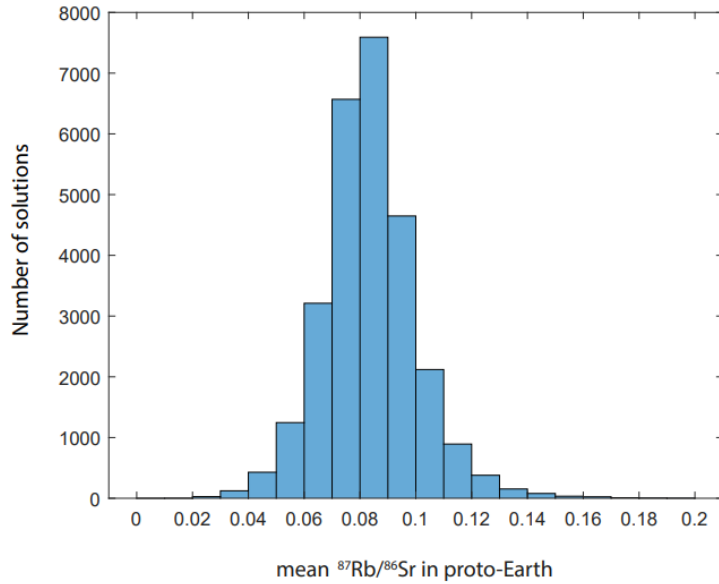
576 **Figure 7**  $^{87}\text{Rb}/^{86}\text{Sr}$  in the accreting proto-Earth as a function of time produced in MonteCarlo  
 577 simulation for solutions that match the criteria described in the main text. Only the final values of  
 578  $^{87}\text{Rb}/^{86}\text{Sr}$  in the bulk silicate Earth range between 0.077 and 0.089.

579

580 This model does not assume that the average  $^{87}\text{Rb}/^{86}\text{Sr}$  of the growing Earth is equal to the  
 581  $^{87}\text{Rb}/^{86}\text{Sr}$  of the BSE. Rather, the  $^{87}\text{Rb}/^{86}\text{Sr}$  can evolve partly independently of the  $^{87}\text{Sr}/^{86}\text{Sr}$  ratio  
 582 in the proto-Earth due to the lack of a closed-system assumption. The only constraint being that at  
 583 the time of the Moon formation, Sr isotopes in the Moon and bulk Silicate Earth equilibrate and  
 584 the  $^{87}\text{Rb}/^{86}\text{Sr}$  ratio of the final Earth is equal to that of the BSE, as shown in Figure 7 that represents  
 585 the  $^{87}\text{Rb}/^{86}\text{Sr}$  ratio of the accreting Earth as a function of time. In Figure 8, we also show the mean  
 586  $^{87}\text{Rb}/^{86}\text{Sr}$  ratio of the final Earth obtained for a series of successful models.

587

588



589

590

591 Figure 8 Histogram of mean  $^{87}\text{Rb}/^{86}\text{Sr}$  ratios (over time) for the Earth that are solutions of the  
 592 MonteCarlo model (section 4.). These ratios range between 0.0137 and 0.260 are both below and  
 593 above the value  $^{87}\text{Rb}/^{86}\text{Sr}_{\text{BSE}}$  (0.077-0.089). This illustrates the open-system behavior of the  
 594 accretion model.

595

596 This model clearly illustrates that our open system model no longer has the constraint that the  
 597 mean  $^{87}\text{Rb}/^{86}\text{Sr}$  is equal to  $^{87}\text{Rb}/^{86}\text{Sr}_{\text{BSE}}$ . Thus, this model simulates more reliably the Earth  
 598 accretion than previously existing model that make assumptions about the building blocks (Mezger  
 599 et al. 2021), or use two component models where the two components evolve as closed system (no  
 600 Rb loss is allowed during accretion; Borg et al. 2022) or assume an  $^{87}\text{Rb}/^{86}\text{Sr}$  ratio equal to that of  
 601 the BSE (Halliday 2008).

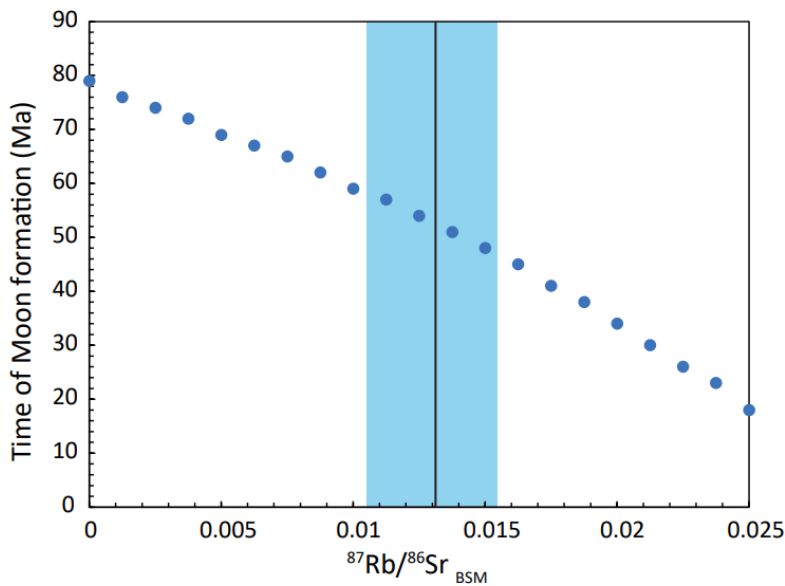
602

603 As there are significant uncertainties in the  $^{87}\text{Rb}/^{86}\text{Sr}$  ratios of the bulk silicate Moon and bulk  
 604 silicate Earth, we assumed a range for these parameters (see discussion above). An evolutionary  
 605 path was considered a successful solution if the  $^{87}\text{Sr}/^{86}\text{Sr}$  ratios of the proto-Earth at the time of  
 606 Moon formation was equal to that of the Moon within error. The most significant source of  
 607 uncertainty in this calculation is the assumed value of the Rb/Sr ratio of the BSM. To investigate  
 608 the influence of this ratio, the age determination was directly calculated for various  $^{87}\text{Rb}/^{86}\text{Sr}$   
 609 values for the Bulk Silicate Moon ranging between that of FAN 60025 (similar to the scenario of

610 Model B) and 0.022 (Model A). This model was also run for the whole range of  $^{87}\text{Rb}/^{86}\text{Sr}$  in the  
611 bulk silicate Earth (0.077-0.089).

612 The results of the MonteCarlo calculation are plotted in Figure 9 and show that the age of Moon  
613 formation ranges between 18 and 79 Ma after CAI for the large range in Rb/Sr assumed for the  
614 BSM and BSE. For  $^{87}\text{Rb}/^{86}\text{Sr}_{\text{BSM}}$  equal to  $0.0135\pm 0.0024$ , as estimated in the Supplementary  
615 materials based on isotope dilution data, the minimum age of lunar formation is  $50.4\pm 6.0$  Ma.

616



617

618 **Figure 9** Determination of the maximum age of Moon formation as a function of the  $^{87}\text{Rb}/^{86}\text{Sr}$   
619 ratio of the bulk Silicate Moon using a MonteCarlo simulation for the  $^{87}\text{Sr}/^{86}\text{Sr}$  ratio of the proto-  
620 Earth as a function of time (see description in section 5.). This simulation takes into account the  
621 joint variability of the parameters shown in Figures 3-4 and the possibly complex open-system Rb-  
622 Sr evolution of the proto-Earth until the Moon forming impact. The blue band marks the preferred  
623  $^{87}\text{Rb}/^{86}\text{Sr}_{\text{BSM}}$  value calculated in this study ( $0.0135\pm 24$ ).

624

625 The results of MonteCarlo simulations in Figure 9 shows that considering all sources of  
626 uncertainties (including  $^{87}\text{Rb}/^{86}\text{Sr}_{\text{BSM}}$ ,  $^{87}\text{Rb}/^{86}\text{Sr}_{\text{BSE}}$ ,  $^{87}\text{Sr}/^{86}\text{Sr}_{\text{FAN}}$  and  $^{87}\text{Sr}/^{86}\text{Sr}_{\text{SS}}$ ), the youngest age  
627 of the Moon should range between 18 and 79 Ma after CAI, depending on the value of  
628  $^{87}\text{Rb}/^{86}\text{Sr}_{\text{BSM}}$ . To illustrate how the improvement in uncertainties affects the calculated results, A  
629 3-D diagram (Figures S2 and S3; Supplementary materials) showing the solutions obtained with  
630 our new data for FAN 60025 can be compared with the solutions obtained with the uncertainties

631 reported in Carlson and Lugmair (1988). The range of solutions is clearly broader with the  
632 uncertainties from Carlson and Lugmair (1988).

633 This approach provides a robust bound on the youngest age of the Moon, independently of  
634 the exact Sr isotope evolution of the proto-Earth, which is currently unknown. Note that our  
635 simulation shows that the Rb/Sr ratio of the BSE has rather small leverage on the calculated age  
636 (see Figure 3) as also demonstrated in section 4.

637 Incidentally, the 60025 FAN anorthosite used for this study with a chronometric age of  
638 4.360 Ga (or 200 Ma after CAI) was used for determining a new Rb-Sr age for the Moon. If there  
639 had been a resetting the Sm-Nd or U-Pb ages, this had probably little effect on the  $^{87}\text{Sr}/^{86}\text{Sr}$  value  
640 of anorthite of FAN 60025, since this mineral phase contains more than 99.95% of Sr in the whole  
641 rock, as this mineral represents 98% of the rock with 40 times more Sr than in the mafic minerals  
642 (Table S2). Thus, our approach that considers the FAN evolution starting from the time of the giant  
643 impact until 4.36 Ga (Model B) does in fact consider implicitly the effect of resetting and our  
644 estimate of  $^{87}\text{Sr}/^{86}\text{Sr}$  at the time of Moon formation depends only on the assumed  $^{87}\text{Rb}/^{86}\text{Sr}$  ratios.

645

## 646 **6. Implications**

647 Our high precision Sr data on lunar rocks implies that the Moon has to have formed earlier  
648 than 79 Ma after the beginning of the Solar System. If we use the preferred value for the  $^{87}\text{Rb}/^{86}\text{Sr}$   
649 ( $=0.0135$ ) of the Bulk Silicate Moon, this value falls to 51 Ma. This age is remarkably close to the  
650 most recent estimate for the earliest age of Moon formation given by Hf-W constraints (Kruijer  
651 and Kleine 2017), assuming again that Earth and Moon were isotopically equilibrated (as evidence  
652 by their similar  $^{182}\text{W}$  abundances, after accounting for differences in the late accreted material).  
653 Using the most recent data for Hf/W ratios in the BSM and BSE, this maximum age is 48 Ma to  
654 obtain a difference between BSM and BSE that does not exceed 15 ppm (Kruijer and Kleine 2017).  
655 These conclusions are clearly at odds with those of Borg et al. (2022) based on the Rb-Sr system.  
656 The difference in our conclusions can be understood as Borg et al. (2022) have not made the  
657 hypothesis that  $^{87}\text{Sr}/^{86}\text{Sr}_{\text{Moon}} = ^{87}\text{Sr}/^{86}\text{Sr}_{\text{BSE}}$  at the time of Moon formation. With this hypothesis, it  
658 is possible for the bulk silicate Earth to evolve to a higher  $^{87}\text{Sr}/^{86}\text{Sr}$  than that of the Moon (see  
659 Figure 5a), and this allows the possibility of delaying the time of Moon formation. Owing to  
660 relaxing the hypothesis of isotope equilibration between Earth and Moon, it is then possible to  
661 obtain younger ages for the Moon. For example, in the Models 6 of (Borg et al., 2022) (see their

662 Table S1 for details) the  $^{87}\text{Sr}/^{86}\text{Sr}_{\text{BSE}}$  at the time of Moon formation ( $=0.699168$ ) can be higher than  
663 that of the BSM ( $=0.699005$ ), which means that the  $^{87}\text{Sr}/^{86}\text{Sr}$  can evolve longer than in the case of  
664 our model. This salient feature of the Borg et al. (2022) model is illustrated in Figure 5a to better  
665 explicit the implications of their hypothesis regarding the absence of Moon-Earth equilibration.  
666 However, as mentioned above this hypothesis is not consistent with the Hf-W and stable isotope  
667 observations (e.g. Fu et al. 2023) and was shown to be very unlikely (Kruijer et al. 2021). This  
668 question was also investigated by Fischer et al. (2021) who also concluded that Earth and Moon  
669 should have equilibrated isotopically after the giant impact.

670 An advantage of our model that differs from that of Borg et al. (2022) is that we consider  
671 a realistic Rb-Sr evolution of the proto-Earth, as it is being accreted. In contrast, Borg et al. (2022)  
672 have assumed a single-stage ‘closed system’ from 1-2 Ma until the time of Moon formation for  
673 both Theia and the proto-Earth. To be more specific, the two components in their model evolve  
674 separately as closed system (after an initial loss of Rb at the beginning of the Solar System). This  
675 means that the accretion process implies no further loss of Rb. This is a strong hypothesis that does  
676 not fit with the idea that the accretion process of the Earth is by essence an open system where  
677 numerous accreting objects of variable Rb/Sr ratios are being added. Such a complex process is  
678 not well described by a single stage evolution.

679 Interestingly, the results of our model are similar to those reported in Mezger et al. (2021)  
680 who reported a formation age for the Moon of  $60\pm 15$  Myr. A notable difference is that our age for  
681 Moon formation represents a minimum age for the Moon, i.e. the Moon did not form later than 79  
682 Ma. It should be mentioned also that the study of Mezger et al. (2021) made strong assumptions  
683 about the proportions and composition of components, one component being volatile-rich (15%)  
684 while the second one was volatile-depleted (85%). However, by considering the trace element data  
685 used to defined these components, one notes that the proportions are not better constrained than  
686 5% (as opposed to the quoted uncertainty of 1%). If one takes these uncertainties into account the  
687 range of ages becomes  $60\pm 30$  Myr. Furthermore, if one uses the mixing proportions (85-15%), to  
688 calculate the  $^{87}\text{Rb}/^{86}\text{Sr}$  of the BSE, one obtains a value of 0.16, which is well above the observed  
689 value ( $\approx 0.08$ ), which makes the reliability of the results problematic. Another issue is that the  
690 history of the FAN 60025 used to derive an age was considered as a fixed value of the initial  
691  $^{87}\text{Sr}/^{86}\text{Sr}$  was considered. As explained in our study, one must also account for the poorly  
692 constrained value of the  $^{87}\text{Rb}/^{86}\text{Sr}$  ratio of the bulk Silicate Moon. If this constraint had been

693 included, the Moon age derived by Mezger et al. (2021) would have been a maximum as in this  
694 study.

695 Our new results are also consistent with the conclusions of Jacobson et al. (2014) who  
696 inferred that the Moon must have formed before at  $95 \pm 32$  Ma after the beginning of the Solar  
697 System.

698 The new Rb-Sr age constraint we propose also puts tighter constraints on the youngest age  
699 of Moon formation and these results may appear inconsistent with a very young age for the Moon  
700 based on recent work on lunar anorthosites or with the model age for Moon accretion given in  
701 Maurice et al. (2020). For example, Borg et al. (2011), measured internal isochrons for the FAN  
702 60025 using the Pb-Pb and Sm-Nd isotope systems and obtained a mean age for this rock of  $4.360$   
703  $\pm 0.003$  Ga (or 208 Ma after CAI). As mentioned above, these authors further argued that if the  
704 lifetime of the magma ocean was short (as calculated in Elkins-Tanton et al., 2011), then the age  
705 of anorthosites would approximately represent the age of Moon formation. This conclusion was  
706 reemphasized based on more age determinations of anorthosites (Boyet et al., 2015). However,  
707 this interpretation has been questioned because it must be ascertained first that the ages of FAN  
708 really record magma ocean crystallization and there is the possibility of resetting the anorthosite  
709 age by a later event (Asphaug, 2014; McLeod et al., 2014). There is also petrological evidence for  
710 a complex history for the anorthosite lunar crust, indicating multiple events associated with  
711 anorthosite formation (Gross et al., 2014).

712 By considering a larger data set, Borg and Carlson (2023) have argued that the concordance  
713 of ages recorded for FAN, urKREEP, Mg-suite rocks as well as the Sm-Nd model age of mare  
714 basalts (Gaffney and Borg 2014) fall within a relatively narrow range between 4.33-4.36 Ga. Given  
715 that the cooling of the magma ocean must be relatively fast, this range of ages for samples from  
716 far distant sites (Borg et al. 2019) cannot be coincidental and must be closely related to the age of  
717 the formation of the Moon. However, given the uncertainties in the ages, the possible range of ages  
718 is actually 4.29-4.38 Ga, which span approximately 100 Ma. This first suggest that the duration of  
719 magmatism presumably associated with the formation of a magma ocean is considerably longer  
720 than assumed by the proponents of a young age for the Moon. The cooling of the lunar magma is  
721 probably extremely fast in its first stages because it is highly convective, so it is unlikely to have  
722 started 100 Ma after the accretion of the Moon. Nevertheless, the formation of a plagioclase lid,  
723 which is unavoidable, will take place after 70% crystallization (Schmidt and Kraettli 2022) and

724 this will considerably slow down the cooling of the lunar mantle. Thermal models that includes  
725 this process show that the formation of the KREEP and FAN reservoirs will take place late  
726 (Maurice et al. 2020). As a result, it is expected that the age of ferro-anorthosites (that start forming  
727 after 70% crystallization) will yield a range of ages reflecting the accumulation of anorthite at the  
728 base of the crust. As shown in Maurice et al. (2020) the duration of the last stages of crystallization  
729 could last up to  $\approx 200$  Ma, due in part to the low thermal conductivity of plagioclase. The recent  
730 ages of KREEP, FAN and the Mg-suite could just reflect this late stage of crystallization.  
731 Furthermore, although the 60025 rock was found at the lunar surface, its breccia texture indicates  
732 that it was excavated from depth by a crater forming impact. The depth of excavation could be  
733 tens of km (e.g. Spudis et al. 1989) which is consistent with its plutonic texture. This means that  
734 anorthosites such as 60025 could have recorded delayed cooling at depth in the lunar crust.

735         Alternatively, it has been shown that the survival of a slushy magma ocean (Michaut and  
736 Neufeld 2022) could lead to a delay in anorthosite crust formation. This model considers first the  
737 formation of a stagnant lid, while the sedimentation of crystals does not take place due to the low  
738 gravity of the Moon and an on-going convection of the slushy and viscous magma ocean. Within  
739 the framework of this scenario, the cooling of the LMO is slowed down and the formation of an  
740 anorthositic crust is delayed by several hundreds of Ma. In brief, both thermal models have the  
741 potential to reconcile the young age of FAN (i.e.  $\approx 200$  Ma after CAI; Borg et al. 2011; Boyet et  
742 al. 2015) with an older age for the Moon, in agreement with our inference based on Rb-Sr.

743  
744         Our Rb-Sr age for the Moon can also be compared with estimates of the Moon accretion  
745 based on U-Pb systematics (Connelly and Bizzarro, 2016; Halliday, 2004). For example, Connelly  
746 and Bizzarro (2016) interpreted the U-Pb fractionation observed between the Earth and its  
747 precursor materials (i.e., chondrites) as reflecting a large-scale event of Pb volatilization during  
748 the Moon-forming impact, thereby dating the age of the Moon with ages ranging between 4.426  
749 and 4.417 Ga, or 141-151 Ma after the beginning of the Solar System, which would seem to  
750 contradict our interpretation of the Rb-Sr record. However, as shown in Rudge et al. (2010),  
751 depending on the conditions of metal-silicate equilibration, on the Pb partitioning in the core  
752 (Wood and Halliday, 2010), or on the choice of U/Pb ratio for representing the bulk silicate Earth  
753 (Halliday, 2004), the constraints provided by U-Pb do not necessarily disagree with our Rb-Sr age.  
754 The U-Pb age constraints were recently reevaluated by Maltese and Mezger (2020). Similar to



755 Ballhaus et al. (2013), these authors showed that the Pb isotope systematics were mostly controlled  
756 by late accretion of volatile rich material that evolved with a high U/Pb ratio due to Pb  
757 incorporation into the Earth core as sulphide (Wood and Halliday, 2010) and this yielded a  
758 preferred age of  $69 \pm 10$  Ma, which seems in agreement with our Rb-Sr constraints. Overall, the  
759 interpretation of U-Pb for the Earth-Moon system are possibly consistent with the Rb/Sr  
760 constraints and is obviously a matter of debate.

761 In summary, our more precise Rb-Sr data for lunar anorthosite 60025 combined with a  
762 model that explores widely various sources of uncertainties and a more realistic accretion model  
763 provides new constraints on the age of the Moon. The main source of uncertainty is now the  
764  $^{87}\text{Rb}/^{86}\text{Sr}$  of the bulk Silicate Moon but based on existing data (compiled in this study), the  
765 youngest age of the Moon would be  $\sim 51$  Ma after the beginning of the Solar System.

766

## 767 References

- 768 Amelin, Y., Kaltenbach, A., Iizuka, T., Stirling, C.H., Ireland, T.R., Petaev, M., Jacobsen, S.B., 2010.  
769 U–Pb chronology of the Solar System’s oldest solids with variable  $^{238}\text{U}/^{235}\text{U}$ . *Earth Planet Sci*  
770 *Lett* 300, 343–350. <https://doi.org/10.1016/J.EPSL.2010.10.015>
- 771 Arnytage, R.M.G., Georg, R.B., Williams, H.M., Halliday, A.N., 2012. Silicon isotopes in lunar  
772 rocks: Implications for the Moon’s formation and the early history of the Earth. *Geochim*  
773 *Cosmochim Acta* 77, 504–514. <https://doi.org/10.1016/j.gca.2011.10.032>
- 774 Asphaug, E., 2014. Impact Origin of the Moon? *Annu Rev Earth Planet Sci* 42, 551–578.  
775 <https://doi.org/10.1146/annurev-earth-050212-124057>
- 776 Ballhaus, C., Laurenz, V., Münker, C., Fonseca, R.O.C., Albarède, F., Rohrbach, A., Lagos, M.,  
777 Schmidt, M.W., Jochum, K.P., Stoll, B., Weis, U., Helmy, H.M., 2013. The U/Pb ratio of the  
778 Earth’s mantle—A signature of late volatile addition. *Earth Planet Sci Lett* 362, 237–245.  
779 <https://doi.org/10.1016/J.EPSL.2012.11.049>
- 780 Barboni, M., Boehnke, P., Keller, B., Kohl, I.E., Schoene, B., Young, E.D., McKeegan, K.D., 2017.  
781 Early formation of the Moon 4.51 billion years ago. *Sci Adv* 3.  
782 <https://doi.org/10.1126/sciadv.1602365>
- 783 Barrat, J.A., Zanda, B., Moynier, F., Bollinger, C., Liorzou, C., Bayon, G., 2012. Geochemistry of CI  
784 chondrites: Major and trace elements, and Cu and Zn Isotopes. *Geochim Cosmochim Acta* 83,  
785 79–92. <https://doi.org/10.1016/j.gca.2011.12.011>
- 786 Barrat, J.A., Zanda, B., Jambon, A., Bollinger, C., 2014. The lithophile trace elements in enstatite  
787 chondrites, *Geochim. Cosmochim. Acta*, 128, 71-94.
- 788 Borg, L.E., Brennecka, G.A., Kruijer, T.S., 2022. The origin of volatile elements in the Earth-Moon  
789 system. *Proc Natl Acad Sci USA* 119, e2115726119.  
790 [https://doi.org/10.1073/PNAS.2115726119/SUPPL\\_FILE/PNAS.2115726119.SAPP.PDF](https://doi.org/10.1073/PNAS.2115726119/SUPPL_FILE/PNAS.2115726119.SAPP.PDF)
- 791 Borg, L.E., Cassata, W.S., Wimpenny, J., Gaffney, A.M., Shearer, C.K., 2020. The formation and  
792 evolution of the Moon’s crust inferred from the Sm-Nd isotopic systematics of highlands rocks.  
793 *Geochim Cosmochim Acta* 290, 312–332. <https://doi.org/10.1016/J.GCA.2020.09.013>
- 794 Borg, L.E., Connelly, J.N., Boyet, M., Carlson, R.W., 2011. Chronological evidence that the Moon is  
795 either young or did not have a global magma ocean. *Nature* 477, 70–73.  
796 <https://doi.org/10.1038/nature10328>

797 Borg, L.E., Gaffney, A.M., Kruijer, T.S., Marks, N.A., Sio, C.K., Wimpenny, J., 2019. Isotopic  
798 evidence for a young lunar magma ocean. *Earth Planet Sci Lett* 523, 115706.  
799 <https://doi.org/10.1016/J.EPSL.2019.07.008>

800 Borg, L.E., Carlson, R.W., 2023. The evolving chronology of Moon formation, *Annu. Rev. Earth*  
801 *Planet. Sci.* 51, 25-52. <https://doi.org/10.1146/annurev-earth-031621-060538>

802 Boyet, M., Carlson, R.W., Borg, L.E., Horan, M., 2015. Sm-Nd systematics of lunar ferroan  
803 anorthositic suite rocks: Constraints on lunar crust formation. *Geochim Cosmochim Acta* 148,  
804 203–218. <https://doi.org/10.1016/j.gca.2014.09.021>

805 Brenan, J.M., Mungall, J.E., Bennett, N.R., 2019. Abundance of highly siderophile elements in lunar  
806 basalts controlled by iron sulfide melt. *Nature Geoscience* 2019 12:9 12, 701–706.  
807 <https://doi.org/10.1038/s41561-019-0426-3>

808 Canup, R.M., 2012. Forming a moon with an Earth-like composition via a giant impact. *Science*  
809 (1979) 338, 1052–1055. <https://doi.org/10.1126/science.1226073>

810 Carlson, R.W., Borg, L.E., Gaffney, A.M., Boyet, M., 2014. Rb-Sr, Sm-Nd and Lu-Hf isotope  
811 systematics of the lunar Mg-suite: The age of the lunar crust and its relation to the time of Moon  
812 formation. *Philosophical Transactions of the Royal Society A: Mathematical, Physical and*  
813 *Engineering Sciences* 372. <https://doi.org/10.1098/rsta.2013.0246>

814 Carlson, R.W., Lugmair, G.W., 1988. The age of ferroan anorthosite 60025: oldest crust on a young  
815 Moon? *Earth Planet Sci Lett* 90, 119–130. [https://doi.org/10.1016/0012-821X\(88\)90095-7](https://doi.org/10.1016/0012-821X(88)90095-7)

816 Charlier, B.L.A., Tissot, F.L.H., Vollstaedt, H., Dauphas, N., Wilson, C.J.N., Marquez, R.T., 2021.  
817 Survival of presolar p-nuclide carriers in the nebula revealed by stepwise leaching of Allende  
818 refractory inclusions. *Sci. Adv* 7.

819 Charnoz, S., Michaut, C., 2015. Evolution of the protolunar disk: Dynamics, cooling timescale and  
820 implantation of volatiles onto the Earth. *Icarus* 260, 440–463.  
821 <https://doi.org/10.1016/j.icarus.2015.07.018>

822 Charnoz, S., Sossi, P.A., Lee, Y.N., Siebert, J., Hyodo, R., Allibert, L., Pignatale, F.C., Landeau, M.,  
823 Oza, A. v., Moynier, F., 2021. Tidal pull of the Earth strips the proto-Moon of its volatiles. *Icarus*  
824 364, 114451. <https://doi.org/10.1016/J.ICARUS.2021.114451>

825 Connelly, J.N., Bizzarro, M., Krot, A.N., Nordlund, Å., Wielandt, D., Ivanova, M.A., 2012. The  
826 absolute chronology and thermal processing of solids in the solar protoplanetary disk. *Science*,  
827 338, 651-655. [10.1126/science.1226919](https://doi.org/10.1126/science.1226919)

828 Connelly, J.N., Bizzarro, M., 2016. Lead isotope evidence for a young formation age of the Earth–  
829 Moon system. *Earth Planet Sci Lett* 452, 36–43. <https://doi.org/10.1016/j.epsl.2016.07.010>

830 Ćuk, M., Stewart, S.T., 2012. Making the moon from a fast-spinning earth: A giant impact followed  
831 by resonant despinning. *Science*, 338, 1047–1052. <https://doi.org/10.1126/science.1225542>

832 Dauphas, N., Burkhardt, C., Warren, P.H., Teng, F.Z., 2014. Geochemical arguments for an Earth-  
833 like Moon-forming impactor. *Philosophical Transactions of the Royal Society A: Mathematical,*  
834 *Physical and Engineering Sciences* 372. <https://doi.org/10.1098/rsta.2013.0244>

835 Day, J.M.D., Pearson, D.G., Taylor, L.A., 2007. Highly siderophile element constraints on accretion  
836 and differentiation of the earth-moon system. *Science* (1979) 315, 217–219.  
837 <https://doi.org/10.1126/science.1133355>

838 Elardo, S.M., Draper, D.S., Shearer, C.K., 2011. Lunar Magma Ocean crystallization revisited: Bulk  
839 composition, early cumulate mineralogy, and the source regions of the highlands Mg-suite.  
840 *Geochim Cosmochim Acta* 75, 3024–3045. <https://doi.org/10.1016/j.gca.2011.02.033>

841 Elkins-Tanton, L.T., Burgess, S., Yin, Q.Z., 2011. The lunar magma ocean: Reconciling the  
842 solidification process with lunar petrology and geochronology. *Earth Planet Sci Lett* 304, 326–  
843 336. <https://doi.org/10.1016/j.epsl.2011.02.004>

844 Fischer-Gödde, M., Kleine, T., 2017. Ruthenium isotopic evidence for an inner solar system origin of  
845 the late veneer. *Nature*, 541:525–527.

846 Fischer, R.A., Zube, N.G., Nimmo, F., 2021. The origin of the Moon's Earth-like tungsten isotopic  
847 composition from dynamical and geochemical modeling, *Nature Comm.* 12, 35-  
848 <https://doi.org/10.1038/s41467-020-2026>

849 Fitoussi, C., Bourdon, B., 2012. Silicon isotope evidence against an enstatite chondrite earth. *Science*  
850 (1979) 335. <https://doi.org/10.1126/science.1219509>

851 Fu, H., Jacobsen, S.B., Sedaghatpour, F., 2023. Moon's high-energy giant-impact origin and  
852 differentiation timeline inferred from Ca and Mg stable isotopes, *Commun. Earth Environ.* 4, 307,  
853 <https://doi.org/10.1038/s43247-023-00974-4>

854 Gaffney, A.M., Borg, L.E., 2014. A young solidification age for the lunar magma ocean. *Geochim.*  
855 *Cosmochim. Acta*, 140:227–240.

856 Gross, J., Treiman, A.H., Mercer, C.N., 2014. Lunar feldspathic meteorites: Constraints on the  
857 geology of the lunar highlands, and the origin of the lunar crust. *Earth Planet Sci Lett* 388, 318–  
858 328. <https://doi.org/10.1016/j.epsl.2013.12.006>

859 Halliday, A.N., 2008. A young Moon-forming giant impact at 70-110 million years accompanied by  
860 late-stage mixing, core formation and degassing of the Earth. *Phil. Trans. Roy. Soc. A*, 366,  
861 4163–4181. <https://doi.org/10.1098/rsta.2008.0209>

862 Halliday, A.N., 2004. Mixing, volatile loss and compositional change during impact-driven accretion  
863 of the Earth. *Nature* 427, 505–509. <https://doi.org/10.1038/nature02275>

864 Halliday, A.N., Porcelli, D., 2001. In search of lost planets - The paleocosmochemistry of the inner  
865 solar system. *Earth Planet Sci Lett* 192, 545–559. [https://doi.org/10.1016/S0012-821X\(01\)00479-4](https://doi.org/10.1016/S0012-821X(01)00479-4)

866

867 Hans, U., Kleine, T., Bourdon, B., 2013. Rb-Sr chronology of volatile depletion in differentiated  
868 protoplanets: BABI, ADOR and ALL revisited. *Earth Planet Sci Lett* 374, 204–214.  
869 <https://doi.org/10.1016/j.epsl.2013.05.029>

870 Hin, R.C., Fitoussi, C., Schmidt, M.W., Bourdon, B., 2014. Experimental determination of the Si  
871 isotope fractionation factor between liquid metal and liquid silicate. *Earth Planet Sci Lett* 387.  
872 <https://doi.org/10.1016/j.epsl.2013.11.016>

873 Hin, R., Coath, C., Carter, P., Nimmo, F., Lai, Y.-J., Pogge von Strandmann, P.A.E., Willbold, M.,  
874 Leinhardt, Z.M., Walter, M.J., Elliott, T., n.d. Magnesium isotope evidence that accretional  
875 vapour loss shapes planetary compositions. *Nature* 549, 511–515.

876 Hofmann, A.W., White, W.M., 1983. Ba, Rb and Cs in the Earth's Mantle. *Zeitschrift fur*  
877 *Naturforschung - Section A Journal of Physical Sciences* 38, 256–266.  
878 <https://doi.org/10.1515/zna-1983-0225>

879 Jacobson, S.A., Morbidelli, A., Raymond, S.N., O'Brien, D.P., Walsh, K.J., Rubie, D.C., 2014. Highly  
880 siderophile elements in Earth's mantle as a clock for the Moon-forming impact. *Nature* 508, 84–  
881 87. <https://doi.org/10.1038/nature13172>

882 Kadlag, Y., Tatzel, M., Frick, D.A., Becker, H., Kühne, P., 2021. In situ Si isotope and chemical  
883 constraints on formation and processing of chondrules in the Allende meteorite, *Geochim.*  
884 *Cosmochim. Acta*, 304, 234-257.

885 Kleine, T., Budde, G., Burkhardt, C., Kruijjer, T.S., Worsham, E.A., Morbidelli, A., Nimmo, F., 2020.  
886 The Non-carbonaceous–Carbonaceous Meteorite Dichotomy. *Space Sci Rev* 216, 1–27.  
887 <https://doi.org/10.1007/S11214-020-00675-W/FIGURES/7>

888 Kleine, T., Hans, U., Irving, A.J.A.J., Bourdon, B., 2012. Chronology of the angrite parent body and  
889 implications for core formation in protoplanets. *Geochim Cosmochim Acta* 84, 186–203.  
890 <https://doi.org/10.1016/j.gca.2012.01.032>

891 König, S., Münker, C., Hohl, S., Paulick, H., Barth, A.R., Lagos, M., Pfänder, J., Büchl, A., 2011.  
892 The Earth's tungsten budget during mantle melting and crust formation. *Geochim Cosmochim*  
893 *Acta* 75, 2119–2136. <https://doi.org/10.1016/j.gca.2011.01.031>

894 Kruijjer, T.S., Archer, G.J., Kleine, T., 2021. No <sup>182</sup>W evidence for early Moon formation. *Nature*  
895 *Geoscience* 2021 14:10 14, 714–715. <https://doi.org/10.1038/s41561-021-00820-2>

896 Kruijer, T.S., Kleine, T., 2017. Tungsten isotopes and the origin of the Moon. *Earth Planet Sci Lett*  
897 475, 15–24. <https://doi.org/10.1016/j.epsl.2017.07.021>

898 Kruijer, T.S., Kleine, T., Fischer-Gödde, M., Sprung, P., 2015. Lunar tungsten isotopic evidence for  
899 the late veneer. *Nature* 520, 534–537. <https://doi.org/10.1038/nature14360>

900 Lock, S.J., Stewart, S.T., 2017. The structure of terrestrial bodies: Impact heating, corotation limits,  
901 and synestias. *J Geophys Res Planets* 122, 950–982. <https://doi.org/10.1002/2016JE005239>

902 Lock, S.J., Stewart, S.T., Petaev, M.I., Leinhardt, Z., Mace, M.T., Jacobsen, S.B., Cuk, M., 2018. The  
903 Origin of the Moon Within a Terrestrial Synestia. *J Geophys Res Planets* 123, 910–951.  
904 <https://doi.org/10.1002/2017JE005333>

905 Maltese, A., Mezger, K., 2020. The Pb isotope evolution of Bulk Silicate Earth: Constraints from its  
906 accretion and early differentiation history. *Geochim Cosmochim Acta* 271, 179–193.  
907 <https://doi.org/10.1016/J.GCA.2019.12.021>

908 Maurice, M., Tosi, N., Schwinger, S., Breuer, D., Kleine, T., 2020. A long-lived magma ocean on a  
909 young Moon. *Sci Adv* 6, eaba8949. <https://doi.org/10.1126/SCIADV.ABA8949>

910 Mezger, K., Maltese, A., Vollstaedt, H., 2021. Accretion and differentiation of early planetary bodies  
911 as recorded in the composition of the silicate Earth, *Icarus*, 365, 114497.

912 McDonough, W.F., Sun, S.S., Ringwood, A.E., Jagoutz, E., Hofmann, A.W., 1992. Potassium,  
913 rubidium, and cesium in the Earth and Moon and the evolution of the mantle of the Earth.  
914 *Geochim Cosmochim Acta* 56, 1001–1012. [https://doi.org/10.1016/0016-7037\(92\)90043-I](https://doi.org/10.1016/0016-7037(92)90043-I)

915 McLeod, C.L., Brandon, A.D., Armytage, R.M.G., 2014. Constraints on the formation age and  
916 evolution of the Moon from <sup>142</sup>Nd-<sup>143</sup>Nd systematics of Apollo 12 basalts. *Earth Planet Sci*  
917 *Lett* 396, 179–189. <https://doi.org/10.1016/j.epsl.2014.04.007>

918 Mougel, B., Moynier, F., Göpel, C., 2018. Chromium isotopic homogeneity between the Moon, the  
919 Earth, and enstatite chondrites. *Earth Planet Sci Lett* 481, 1–8.  
920 <https://doi.org/10.1016/j.epsl.2017.10.018>

921 Moynier, F., Day, J., Wataru, O., Yokoyama, T., Day, J.M.D., Okui, W., Bouvier, A., Walker, R.J.,  
922 Podosek, F.A., 2012. Planetary-scale strontium isotopic heterogeneity and the age of volatile  
923 depletion of early Solar System materials. Article in *The Astrophysical Journal* 758, 45.  
924 <https://doi.org/10.1088/0004-637X/758/1/45>

925 Münker, C., 2010. A high field strength element perspective on early lunar differentiation. *Geochim.*  
926 *Cosmochim. Acta* 74, 7340–7361. <https://doi.org/10.1016/j.gca.2010.09.021>

927 Murthy, V.R., Evensen, N.M., Jahn, B.M., Coscio, M.R., 1971. Rb-Sr ages and elemental abundances  
928 of K, Rb, Sr, and Ba in samples from the Ocean of Storms. *Geochim. Cosmochim. Acta* 35,  
929 1139–1153. [https://doi.org/10.1016/0016-7037\(71\)90030-5](https://doi.org/10.1016/0016-7037(71)90030-5)

930 Nakajima, M., Stevenson, D.J., 2014. Investigation of the initial state of the Moon-forming disk:  
931 Bridging SPH simulations and hydrostatic models. *Icarus* 233, 259–267.  
932 <https://doi.org/10.1016/j.icarus.2014.01.008>

933 O’Brien, D.P., Walsh, K.J., Morbidelli, A., Raymond, S.N., Mandell, A.M., 2014. Water delivery and  
934 giant impacts in the ‘Grand Tack’ scenario. *Icarus* 239, 74–84.  
935 <https://doi.org/10.1016/J.ICARUS.2014.05.009>

936 Pahlevan, K., Stevenson, D.J., 2007. Equilibration in the aftermath of the lunar-forming giant impact.  
937 *Earth Planet Sci Lett* 262, 438–449. <https://doi.org/10.1016/j.epsl.2007.07.055>

938 Papanastassiou, D.A., Wasserburg, G.J., 1978. Strontium isotopic anomalies in the Allende Meteorite.  
939 *Geophys Res Lett* 5, 595–598. <https://doi.org/10.1029/GL005I007P00595>

940 Paquet, M., Day, J.M.D., Brown, D.B., Waters, C.L., 2022. Effective global mixing of the highly  
941 siderophile elements into Earth’s mantle inferred from oceanic abyssal peridotites, *Geochim.*  
942 *Cosmochim. Acta*, 316, 347-362.

943 Philpotts, J.A., Schnetzler, C.C., 1970. Potassium, rubidium, strontium, barium, and rare-earth  
944 concentrations in lunar rocks and separated phases. *Science*, 167, 493–495.  
945 <https://doi.org/10.1126/science.167.3918.493>

946 Philpotts, J.A., Schnetzler, C.C., Bottino, M.L., Schuhmann, S., Thomas, H.H., 1972. Luna 16: Some  
947 Li, K, Rb, Sr, Ba, rare-earth, Zr, and Hf concentrations. *Earth Planet Sci Lett* 13, 429–435.  
948 [https://doi.org/10.1016/0012-821X\(72\)90120-3](https://doi.org/10.1016/0012-821X(72)90120-3)  
949 Righter, K., Boujibar, A., Humayun M., Yang, S., Rowland II, R., Pando, K., 2023. Activity model  
950 for 36 elements in Fe-Ni-Si-SC liquids with application to terrestrial planet accretion and mantle  
951 geochemistry: New data for Ru, Re, Pt, Os, Ti, Nb, and Ta, *Geochim. Cosmochim. Acta*, 354,  
952 211-228.

953 Ringwood, A.E., Kesson, S.E., 1977. Basaltic magmatism and the bulk composition of the moon - II.  
954 Siderophile and Volatile Elements in Moon, Earth and Chondrites: Implications for Lunar  
955 Origin. *The Moon* 16, 425–464. <https://doi.org/10.1007/BF00577902>  
956 Rotenberg, E., Davis, D.W., Amelin, Y., Ghosh, S., & Bergquist, B.A., 2012. Determination of the  
957 decay-constant of <sup>87</sup>Rb by laboratory accumulation of <sup>87</sup>Sr. *Geochim. Cosmochim. Acta*, 85, 41–  
958 57. <https://doi.org/10.1016/J.GCA.2012.01.016>  
959 Rudge, J.F., Kleine, T., Bourdon, B., 2010. Broad bounds on Earths accretion and core formation  
960 constrained by geochemical models. *Nat Geosci* 3. <https://doi.org/10.1038/ngeo872>  
961 Schiller, M., Bizzarro, M., Fernandes, V.A., 2018. Isotopic evolution of the protoplanetary disk and  
962 the building blocks of Earth and the Moon. *Nature* 555, 501–510.  
963 <https://doi.org/10.1038/nature25990>  
964 Schmidt, M.W., Kraetli, G., 2022. Experimental crystallization of the lunar magma ocean, initial  
965 selenotherm and density stratification, and implications for crust formation, overturn and the  
966 bulk silicate Moon composition. *J. Geophys. Res.*, 127, e2022JE007187. <https://doi.org/10.1029/2022JE007187>  
967  
968 Schnetzler, C.C., Nava, D.F., 1971. Chemical composition of Apollo 14 soils 14163 and 14259. *Earth  
969 Planet Sci Lett* 11, 345–350. [https://doi.org/10.1016/0012-821X\(71\)90191-9](https://doi.org/10.1016/0012-821X(71)90191-9)  
970 Sedaghatpour, F., Teng, F.Z., Liu, Y., Sears, D.W.G., Taylor, L.A., 2013. Magnesium isotopic  
971 composition of the Moon. *Geochim Cosmochim Acta* 120, 1–16.  
972 <https://doi.org/10.1016/j.gca.2013.06.026>  
973 Shahar, A., Hillgren, V.J., Young, E.D., Fei, Y., Macris, C.A., Deng, L., 2011. High-temperature Si  
974 isotope fractionation between iron metal and silicate, *Geochim. Cosmochim. Acta*, 75, 7688-  
975 7697

976 Sprung, P., Kleine, T., Scherer, E.E., 2013. Isotopic evidence for chondritic Lu/Hf and Sm/Nd of the  
977 Moon. *Earth Planet. Sci. Lett.* 380:77-87.

978 Stracke, A., Palme, H., Gellissen, M., Münker, C., Kleine, T., Birbaum, K., Günther, D., Bourdon, B.,  
979 Zipfel, J., 2012. Refractory element fractionation in the Allende meteorite: Implications for solar  
980 nebula condensation and the chondritic composition of planetary bodies. *Geochim Cosmochim  
981 Acta* 85. <https://doi.org/10.1016/j.gca.2012.02.006>  
982 Taylor, D.J., McKeegan, K.D., Harrison, T.M., 2009. Lu–Hf zircon evidence for rapid lunar  
983 differentiation. *Earth Planet. Sci. Lett.* 279:157–64.

984 Thiemens, M.M., Sprung, P., Fonseca, R.O.C., Leitzke, F.P., Münker, C., 2019. Early Moon  
985 formation inferred from hafnium–tungsten systematics. *Nat Geosci* 12, 696–700.  
986 <https://doi.org/10.1038/s41561-019-0398-3>  
987 Thommes, E.W., Duncan, M.J., Levison, H.F., 2003. Oligarchic growth of giant planets. *Icarus*.  
988 [https://doi.org/10.1016/S0019-1035\(02\)00043-X](https://doi.org/10.1016/S0019-1035(02)00043-X)  
989 Touboul, M., Kleine, T., Bourdon, B., Palme, H., Wieler, R., 2007. Late formation and prolonged  
990 differentiation of the Moon inferred from W isotopes in lunar metals. *Nature* 450.  
991 <https://doi.org/10.1038/nature06428>  
992 Touboul, M., Puchtel, I.S., Walker, R.J., 2015. Tungsten isotopic evidence for disproportional late  
993 accretion to the Earth and Moon. *Nature* 520, 530–533. <https://doi.org/10.1038/nature14355>  
994 Trinquier, A., Birck, J.L., Allègre, C.J., 2007. Widespread <sup>54</sup>Cr heterogeneity in the inner solar system  
995 *Astrophys. J.* 655, 1179—1185.

- 996 Trinquier, A., Elliott, T., Ulfbeck, D., Coath, C., Krot, A.N., Bizzarro, M., 2009. Origin of  
997 nucleosynthetic isotope heterogeneity in the solar protoplanetary disk, *Science*, 324, 374–376.  
998 Walker, R.J., 2009. Highly siderophile elements in the Earth, Moon and Mars: Update and  
999 implications for planetary accretion and differentiation. *Chemie der Erde* 69, 101–125.  
1000 <https://doi.org/10.1016/j.chemer.2008.10.001>  
1001 Wood, B.J., Halliday, A.N., 2010. The lead isotopic age of the Earth can be explained by core  
1002 formation alone. *Nature* 465, 767–770. <https://doi.org/10.1038/nature09072>  
1003 Yobregat, E., Fitoussi, C., Bourdon, B., 2017. A new method for TIMS high precision analysis of Ba  
1004 and Sr isotopes for cosmochemical studies. *J Anal At Spectrom* 32.  
1005 <https://doi.org/10.1039/c7ja00012j>  
1006 Young, E.D., Kohl, I.E., Warren, P.H., Rubie, D.C., Jacobson, S.A., Morbidelli, A., 2016. Oxygen  
1007 isotopic evidence for vigorous mixing during the Moon-forming giant impact. *Science* (1979)  
1008 351, 493–496. <https://doi.org/10.1126/science.aad0525>  
1009 Zhang, B., Lin, Y., Moser, D.E., Hao, J., Liu, Y., Zhang, J., Barker, I.R., Li, Q., Shieh, S.R., Bouvier,  
1010 A., 2021. Radiogenic Pb mobilization induced by shock metamorphism of zircons in the Apollo  
1011 72255 Civet Cat norite clast. *Geochim Cosmochim Acta* 302, 175–192.  
1012 <https://doi.org/10.1016/J.GCA.2021.03.012>  
1013 Zhang, J., Dauphas, N., Davis, A.M., Leya, I., Fedkin, A., 2012. The proto-Earth as a significant  
1014 source of lunar material. *Nat Geosci* 5, 251–255. <https://doi.org/10.1038/ngeo1429>  
1015  
1016

1017 **Acknowledgements:** We thank the NASA curatorial staff for giving us access to the Apollo lunar  
1018 samples, Guillaume Caro, Chloé Michaut, Stéphane Labrosse and Herbert Palme for discussions,  
1019 and Philippe Telouk for maintaining the TRITON in good operation. We thank Richard Carlson  
1020 and an anonymous reviewer for their insightful comments that helped improve the manuscript.

1021 **Funding:** This study was funded both by the ANR project ISOVOL (ANR-12-BS06-0002) and by  
1022 the Labex LIO (ANR-10-LABX-0066) and received partial support from the ERC project  
1023 COSMOKEMS (#694819).  
1024

1025 **Author contributions:** EY: Investigation, conceptualization, writing. CF: Funding acquisition,  
1026 conceptualization, writing. BB: Funding acquisition, conceptualization, writing, formal analysis.  
1027  
1028  
1029  
1030  
1031  
1032  
1033  
1034  
1035

1036 **Supplementary materials**

1037

1038 **1. Radioactive correction in FAN 60025 for deriving the initial  $^{87}\text{Sr}/^{86}\text{Sr}$  at 4.36 Ga**

1039 **2. Calculation of the condensation temperature of Sr and W in the conditions of Moon**  
1040 **formation**

1041 **3. Additional figures**

1042

1043

1044 **1. Radioactive correction in FAN 60025 for deriving the initial  $^{87}\text{Sr}/^{86}\text{Sr}$  at 4.36 Ga**

1045 One question that arises is whether this sample has remained a closed system since its formation  
1046 dated at  $4.360 \pm 3$  Ga using the Sm-Nd and U-Pb systems (Borg et al. 2011). As shown in Borg et  
1047 al. (2011) and Carlson and Lugmair (1988), the mineral separates analyzed in this sample plot on  
1048 an isochron that are indicative of a closed-system behavior for the Sm/Nd and U/Pb systems.  
1049 Nevertheless, it is worth investigating whether a more complex history for Rb-Sr systematics in  
1050 this rock is possible. To explore the maximum possible uncertainties, we consider two extreme  
1051 scenarios.

1052 First, one could consider that the Rb contained in the sample was added late and to obtain the  
1053 maximum effect, it would have to be added at the last minute (no in-growth of  $^{87}\text{Sr}$ ). In this case,  
1054 the measured  $^{87}\text{Sr}/^{86}\text{Sr}$  ratio would have evolved with  $\text{Rb}/\text{Sr} = 0$ . The age of the Moon was  
1055 recalculated and the results are plotted in Figure S4.

1056 Second, in this case, we consider that the FAN 60025 has evolved with a higher Rb that was  
1057 recently lost. The maximum Rb/Sr ratio that one could consider is that it was equal to  
1058  $^{87}\text{Rb}/^{86}\text{Sr}_{\text{BSM}} = 0.014 - 0.022$ . In this case the calculated initial  $^{87}\text{Sr}/^{86}\text{Sr}$  at 4.36 Ga ranges between  
1059 0.69820217 and 0.69769987, which is below the value of the initial  $^{87}\text{Sr}/^{86}\text{Sr}$  for the inner Solar  
1060 System. Thus, this second scenario is considered even more unlikely.

1061

1062 **2. Calculation of the condensation temperature of Sr and W in the conditions of Moon**  
1063 **formation**

1064 In order to provide further arguments for the isotope equilibration between the Moon and the bulk  
1065 Silicate Earth after the giant impact, the 50% condensation temperatures of Ca, Sr and W were  
1066 calculated using the formalism described in Ivanov et al. (2022) using the FactSage™ software.  
1067 The composition of the bulk Silicate Earth given in Ivanov et al. (2022) was used. Fegley et al.

1068 (2023) have assumed that the activity coefficient of Sr was equal to 1. However, the software used  
1069 here (FactSage™) includes in its data base a comprehensive data set especially developed for Sr,  
1070 based on the PhD work of Shukla (2012) who has studied several binary and ternary compositions  
1071 including Sr yielding an activity coefficient different from 1.

1072 The 50% condensation temperature was calculated for various pressures ranging between 10 bar  
1073 and 0.001 bar, corresponding to the conditions in the proto-lunar (or synestia) disk as described in  
1074 Lock et al. (2018). The results are depicted in Figure 1 and clearly show that the condensation  
1075 temperatures for the three elements are relatively close to each other. Thus, if there has been Ca  
1076 and W isotope equilibration between the Moon and the bulk Silicate Earth, this must have been  
1077 the case for Sr as well.

1078



1079

1080 **Table S1.  $^{87}\text{Sr}/^{86}\text{Sr}$  ratios in NIST SRM 987**

<b>Standards</b>	<b><math>^{87}\text{Sr}/^{86}\text{Sr}</math></b>	<b>2 SE</b>	<b>2SE (ppm)</b>	<b>N blocks</b>
std 1	0.7102485	0.0000014	2.0	986
std 2	0.7102487	0.0000015	2.2	957
std 3	0.7102501	0.0000012	1.7	616
std 4	0.7102477	0.0000013	1.8	564
std 5	0.7102478	0.0000013	1.8	417
std 6	0.7102504	0.0000010	1.5	971
std 7	0.7102483	0.0000011	1.6	798
std 8	0.7102482	0.0000012	1.7	1021
std 9	0.7102491	0.0000013	1.8	594
std 10	0.7102491	0.0000012	1.7	558
std 11	0.7102486	0.0000011	1.6	697
std 12	0.7102498	0.0000011	1.5	991
std 13	0.7102476	0.0000014	1.9	767
std 14	0.7102490	0.0000012	1.7	983
std 15	0.7102482	0.0000012	1.6	552
		2SD	2SD (ppm)	
<b>Mean</b>	0.7102487	0.0000017	2.4	15

1081

1082

1083

1084

1085

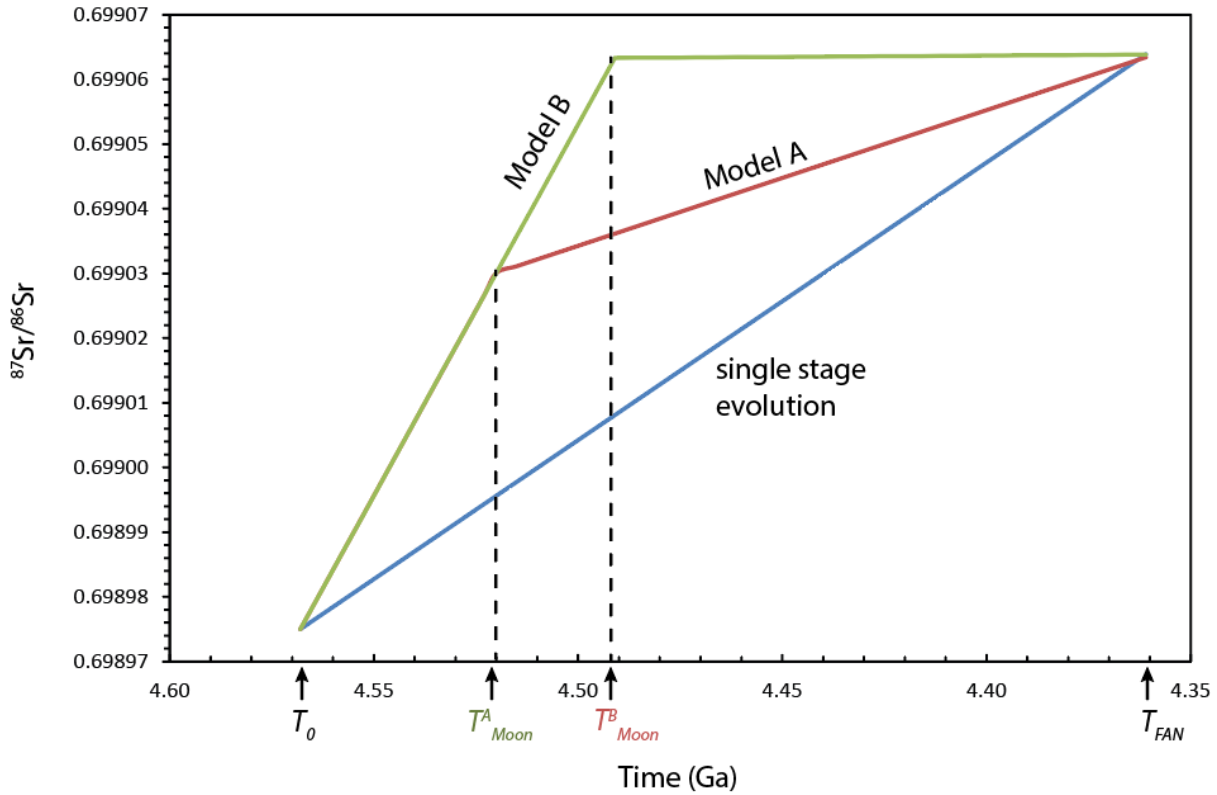
1086

**Table S2 Values of input parameters in MonteCarlo simulations**

Input parameter	Description	Range
$M_0$	Initial mass of protoEarth	1-1000 km radius
$f_{Sr}^i$	Relative incremental mass accreted at stage i	0-1
$^{87}\text{Rb}/^{86}\text{Sr}_{\text{BSM}}$	Parent daughter ratio bulk silicate Moon	0.00027-0.022
$^{87}\text{Rb}/^{86}\text{Sr}_{\text{BSE}}$	Parent daughter ratio bulk silicate Earth	0.077-0.089
$^{87}\text{Sr}/^{86}\text{Sr}_{\text{Solar System}}$	Initial ratio of Solar System measured in CAI	0.698978
$T_{\text{Moon}}$	Age of Moon formation	0-200 Ma

1087

1088



1089

1090 Figure S1

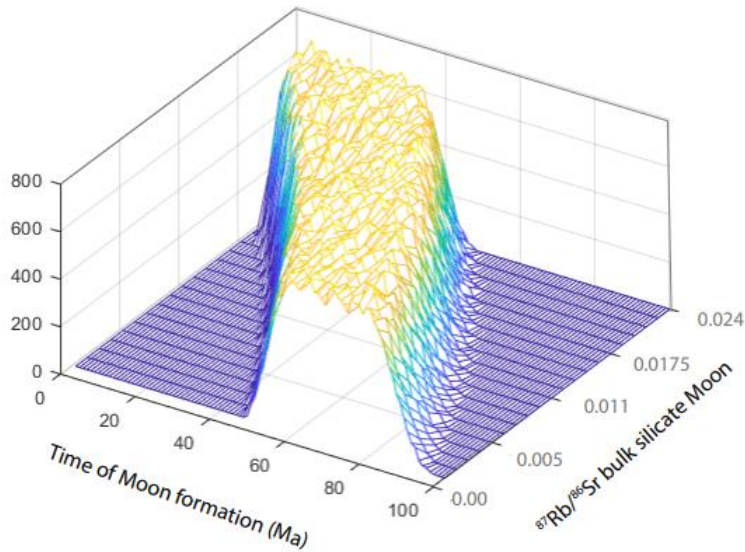
1091 Evolution of the  $^{87}\text{Sr}/^{86}\text{Sr}$  ratios for ferroanorthosite 60025 as a function of time for Model A and  
 1092 Model B compared with a single stage evolution starting from the beginning of the Solar System  
 1093 at  $T_0$  as described in Carlson et al., (2014) and Carlson and Lugmair, (1988). Model A and Model  
 1094 B both assume that the Moon and bulk Silicate Earth had similar  $^{87}\text{Sr}/^{86}\text{Sr}$  at the time of Moon  
 1095 formation ( $T_{\text{Moon}}^A$  and  $T_{\text{Moon}}^B$ ) which is not the case of the single stage model. The  $^{87}\text{Rb}/^{86}\text{Sr}$  of the  
 1096 bulk silicate Moon or the FAN 60025 (given by the slope of the evolution lines) are much lower  
 1097 than in the single stage model. The first stage of  $^{87}\text{Sr}/^{86}\text{Sr}$  evolution had a chondritic  $^{87}\text{Rb}/^{86}\text{Sr}$   
 1098 (green line), the second stage had a  $^{87}\text{Rb}/^{86}\text{Sr}=0.014$  for model A (red line) and  $^{87}\text{Rb}/^{86}\text{Sr}=2.8 \times 10^{-4}$   
 1099 for model B (flat green line).

1100

1101

1102

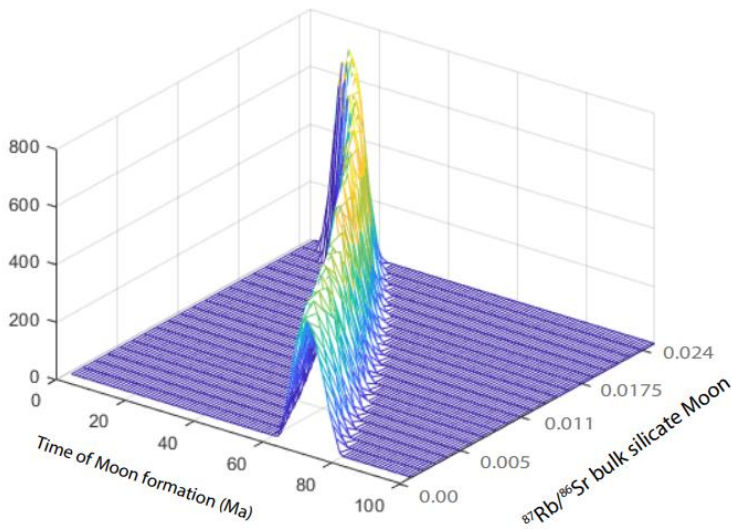
1103



1104

1105

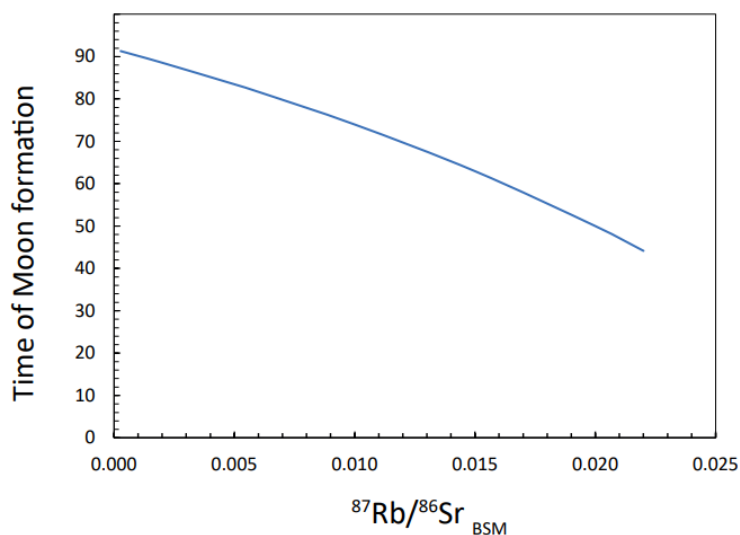
1106 Figure S2 MonteCarlo solutions obtained for the age of the Moon versus  $^{87}\text{Rb}/^{86}\text{Sr}$  in the bulk silicate Moon. The  
1107 vertical axis represents the number of solutions. In this calculation, the uncertainty in the  $^{87}\text{Sr}/^{86}\text{Sr}$  ratio of FAN 60025  
1108 is that measured obtained by Carlson and Lugmair (1988) i.e. 28 ppm.



1109

1110 Figure S3 MonteCarlo solutions obtained for the age of the Moon versus  $^{87}\text{Rb}/^{86}\text{Sr}$  in the bulk silicate Moon. The  
1111 vertical axis represents the number of solutions. In this calculation, the uncertainty in the  $^{87}\text{Sr}/^{86}\text{Sr}$  ratio of FAN 60025  
1112 is that measured in this study (2.4 ppm). The age range of solutions is far more restricted in this second case, which  
1113 illustrates the benefit of the more precise measurement in constraining the age of the Moon.

1114



1115  
 1116 Figure S4 Forward model for the calculation of the age of the Moon based on Rb-Sr isotope  
 1117 systematics assuming that the Rb in FAN 60025 was not indigenous (i.e. added at the last minute).  
 1118 We consider this hypothesis unlikely as FAN 60025 shows isochrons for three isotope systems  
 1119 and the 60025 plagioclase falls on a Rb-Sr isochron defined with other FANs (Shih et al. 2005).

1120  
 1121

#### 1122 **References**

- 1123 Borg, L.E., Connelly, J.N., Boyet, M., Carlson, R.W., 2011. Chronological evidence that the Moon is either young or  
 1124 did not have a global magma ocean. *Nature* 477, 70–73. <https://doi.org/10.1038/nature10328>  
 1125 Carlson, R.W., Borg, L.E., Gaffney, A.M., Boyet, M., 2014. Rb-Sr, Sm-Nd and Lu-Hf isotope systematics of the lunar  
 1126 Mg-suite: The age of the lunar crust and its relation to the time of Moon formation. *Phil. Trans. Roy. Soc. A* 372.  
 1127 <https://doi.org/10.1098/rsta.2013.0246>  
 1128 Carlson, R.W., Lugmair, G.W., 1988. The age of ferroan anorthosite 60025: oldest crust on a young Moon? *Earth Planet*  
 1129 *Sci Lett* 90, 119–130. [https://doi.org/10.1016/0012-821X\(88\)90095-7](https://doi.org/10.1016/0012-821X(88)90095-7)  
 1130 Fegley, Jr, B., Lodders, K., Jacobson, N.S., 2023. Chemical equilibrium calculations for bulk silicate earth material at  
 1131 high temperatures, *Geochemistry* 83, 125961. <https://doi.org/10.1016/j.chemer.2023.125961>  
 1132 Ivanov, D., Fitoussi, C., Bourdon, B., 2022. Trace element volatility and the conditions of liquid-vapor separation in  
 1133 the proto-lunar disk, *Icarus* 386, 115143. <https://doi.org/10.1016/j.icarus.2022.115143>  
 1134 Lock, S.J., Stewart, S.T., Petaev, M.I., Leinhardt, Z., Mace, M.T., Jacobsen, S.B., Cuk, M., 2018. The Origin of the  
 1135 Moon Within a Terrestrial Synestia. *J Geophys Res Planets* 123, 910–951. <https://doi.org/10.1002/2017JE005333>  
 1136 Shih, C.Y., Nyquist, L.E., Reese, Y., Yamaguchi, A., Takeda, H., 2005. Rb-Sr and Sm-Nd Isotopic Studies of Lunar  
 1137 Highland Meteorite Y86032 and Lunar Ferroan Anorthosites 60025 and 67075. 36th Annual Lunar Planet. Sci.  
 1138 Conf., 1433.  
 1139 Shukla (2012) Development of a Critically Evaluated Thermodynamic Database for the Systems Containing Alkaline-  
 1140 Earth Oxides, PhD Thesis, Ecole Polytechnique, Montreal, 350 pp. [https://central.bac-](https://central.bac-lac.gc.ca/.item?id=NR91235&op=pdf&app=Library&is_thesis=1&oclc_number=1019464323)  
 1141 [lac.gc.ca/.item?id=NR91235&op=pdf&app=Library&is\\_thesis=1&oclc\\_number=1019464323](https://central.bac-lac.gc.ca/.item?id=NR91235&op=pdf&app=Library&is_thesis=1&oclc_number=1019464323)

1142  
 1143